Control of pili synthesis and putrescine homeostasis in *Escherichia coli*

Running title: *E. coli* surface motility and putrescine homeostasis

Iti Mehta[1#], Jacob Hogins[1#], Sydney Hall[1], Gabrielle Vragel[1], Sankalya Ambagaspitiye[1Δ], Philippe Zimmern[2], Larry Reitzer[1]*

[1] Department of Biological Sciences, The University of Texas at Dallas, Richardson, Texas

[2] Department of Urology, University of Texas Southwestern Medical Center, Dallas, Texas, USA

[Δ] Current address: Department of Biosystems Technology, Faculty of Technology, University of Sri Jayewardenepura, Homagama, 10206, Sri Lanka.

*Author for correspondence: Tel: 972-883-2502; Fax: 972-883-2409; reitzer@utdallas.edu

# Authors contributed equally and should be considered co-first authors

Keywords: polyamines, putrescine, surface motility, pili, *Escherichia coli*, putrescine homeostasis

Summary

Polyamines are biologically ubiquitous cations that bind to nucleic acids, ribosomes, and phospholipids and, thereby, modulate numerous processes, including surface motility in *Escherichia coli*. We characterized the metabolic pathways that contribute to polyamine-dependent control of surface motility in the commonly used strain W3110 and the transcriptome of a mutant lacking a putrescine synthetic pathway that was required for surface motility. Genetic analysis showed that surface motility required type 1 pili, the simultaneous presence of two independent putrescine anabolic pathways, and modulation by putrescine transport and catabolism. An immunological assay for FimA—the major pili subunit, reverse transcription quantitative PCR of *fimA*, and transmission electron microscopy confirmed that pili synthesis required putrescine. Comparative RNAseq analysis of a wild type and Δ*speB* mutant which exhibits impaired pili synthesis showed that the latter had fewer transcripts for pili structural genes and for *fimB* which codes for the phase variation recombinase that orients the *fim* operon promoter in the ON phase, although loss of *speB* did not affect the promoter orientation. Results from the RNAseq analysis also suggested (a) changes in transcripts for several transcription factor genes that affect *fim* operon expression, (b) compensatory mechanisms for low putrescine which implies a putrescine homeostatic network, and (c) decreased transcripts of genes for oxidative energy metabolism and iron transport which a previous genetic analysis suggests may be sufficient to account for the pili defect in putrescine synthesis mutants. We conclude that pili synthesis requires putrescine and putrescine concentration is controlled by a complex homeostatic network that includes the genes of oxidative energy metabolism.

38 ## Introduction

39 Polyamines are flexible aliphatic cations that are found in virtually all organisms. *E. coli*
40 contains putrescine (1,4-diaminobutane) and lesser amounts of spermidine (N-(3-aminopropyl)-
41 1,4-diaminobutane), and cadaverine (1,5-diaminopentane) (1, 2). Both the pathways and enzymes
42 of polyamine synthesis are redundant (Figure 1). Strains that lack eight of these genes do not
43 contain detectable polyamines, grow slowly aerobically, and do not grow anaerobically (3).
44 Polyamines interact with nucleic acids and phospholipids, can affect chromosome and ribosome
45 structure, ribosome-mRNA interactions, and protein and nucleic acid elongation rates (4).
46 Polyamines modulate, but are not required for, protein synthesis (5) and expression of hundreds of
47 genes (6). A major mechanism of polyamine-dependent regulation is translational control of genes
48 for 18 major transcription regulators: four of the seven σ factors – σ^{18} (FecI), σ^{24} (RpoE), σ^{38}
49 (RpoS), and σ^{54} (RpoN); three histone-like DNA-binding proteins (Fis, H-NS, and StpA); and
50 CpxR, Cya, Cra, and UvrY (5, 6).

51 Polyamines control flagella-dependent surface motility of *Proteus mirabilis* and pili-
52 dependent surface motility (PDSM) of *E. coli*: the latter has been reported to require the polyamine
53 spermidine (7, 8). While reconstructing putrescine-deficient strains to characterize the basis for
54 the anaerobic growth defect, we noticed that a mutant unable to synthesize spermidine moved
55 normally, while mutants lacking enzymes of putrescine synthesis moved poorly. We characterized
56 the role of polyamines on *E. coli* surface motility and pili synthesis by genetic analysis, ELISA
57 assays, RT-qPCR, electron microscopy, and RNAseq. We showed that PDSM and pili synthesis
58 required two independent pathways of putrescine synthesis, but did not require spermidine, and
59 was modulated by putrescine transport and catabolism. Results from an RNAseq analysis are

60 consistent with multiple mechanisms of putrescine-dependent control, and, unexpectedly, suggests
61 a putrescine homeostatic network that rewires metabolism to maintain intracellular putrescine.
62

63 ## Results

64 **W3110 surface motility requires pili**

65 An assessment of surface motility for *E. coli* K-12 and eight derivatives showed five strains
66 covered a plate in 12-18 hours, while four did not traverse a plate in 36 hours (9). The slow-moving
67 strains generated genetically stable fast-moving variants which suggests that the former were
68 ancestral. We chose our lab strain of W3110 for further study because (a) it exhibited the least
69 variability in spreading diameter and generated fewer fast-moving variants, and (b) we had
70 previously analyzed this strain for the energy requirements for surface motility (10). We refer to
71 our slow-moving lab strain hereafter as W3110 but not all W3110 strains move similarly: the
72 W3110 from the genetic stock center is a fast-moving variant (9).

73 Several results suggested that W3110 requires pili for surface motility. First, deletion of
74 *fimA*, which codes for the major type 1 pili subunit, abolished the oscillatory pattern and reduced,
75 but did not eliminate, surface motility, but deletion of *fliC* which encodes the major flagellum
76 subunit did not affect surface motility (Figure 2A). Second, electron microscopy confirmed that
77 W3110 isolated from surface motility plates possessed pili (Figure 2B). None of >500 cells
78 expressed flagella. A mixed population of elongated (3-4 μm) and non-elongated (<2 μm) cells
79 were visible, and pili were mostly associated with elongated cells. Finally, W3110 surface motility
80 requires glucose (10) which should prevent flagella synthesis via inhibition of cyclic AMP
81 synthesis (11). We confirmed that glucose suppressed swimming motility which implies
82 suppression of flagella synthesis in W3110 during surface motility assays (Figure 2C). A W3110

83 derivative with deletions of both *fliC* and *fimA* still exhibited outward movement on a surface
84 motility plate (Figure 2A), but electron microscopy showed the absence of appendages (Figure
85 2C). In summary, genetics, electron microscopy, and a glucose requirement show that W3110
86 surface motility requires pili.

87 Results from W3110 sequencing found an *IS1* insertion in *fimE* which could explain its
88 greater movement that is less variable and greater genetic stability. The FimB and FimE
89 recombinases are the major components of phase variation that determines the orientation of the
90 promoter that initiates transcription of the *fimAICDFGH* operon which codes for the pili structural
91 proteins. The FimB recombinase favors the productive ON orientation, while the more active FimE
92 recombinase favors the unproductive OFF orientation (12-14). The insertion in *fimE* is the likely
93 basis for the relative stability of W3110.

94

95 **PDSM required two independent putrescine synthesis pathways.**

96 We examined PDSM requirements for polyamine anabolic pathways. A major putrescine
97 biosynthetic pathway is ornithine decarboxylation either by the constitutive SpeC or the low-pH
98 inducible SpeF. The Δ*speC* and Δ*speF* mutants moved as well as the parental strain, but a Δ*speC*
99 Δ*speF* double mutant moved less well (Figure 3). SpeA (arginine decarboxylase) and SpeB
100 (agmatinase) catalyze an alternate two-step putrescine synthetic pathway (Figure 1) (15): deletion
101 of either gene reduced surface motility (Figure 3). The Δ*speA*, Δ*speB*, and Δ*speC* Δ*speF* strains
102 grew as well as the parental strain (Supplemental Figure 1A) and had normal swimming motility
103 (Supplemental Figure 1B). A Δ*speE* mutant, which lacks the enzyme for spermidine synthesis,
104 moved on a surface as well as the parental strain (Figure 3).

105 Supplemental putrescine at 1 mM restored surface motility of a *speB* mutant (Figure 4A)
106 and a *speA* mutant (not shown). Spermidine did not restore wild type movement and, also, caused
107 an unusual pattern of movement in the parental strain (Figure 4A). These exogenous concentrations
108 of putrescine and spermidine had no effect on growth rates in liquid motility medium (not shown).
109 In summary, PDSM required the simultaneous presence of two independent pathways of putrescine
110 synthesis but did not require spermidine.
111
112 **Loss of putrescine transport systems affected surface motility.**
113 *E. coli* has several polyamine transport systems and one has been reported to require for
114 surface motility (16, 17). Mutants lacking the PlaP and PotF putrescine transporters had 50% and
115 40% reduced surface motility, respectively, and lost the concentric ring pattern (Figure 5A). Loss
116 of the PotE and PuuP transporters affected neither the movement diameter (Figure 5B) nor
117 concentric ring formation (Figure 5A). We note that *potF* and *plaP* are more highly expressed than
118 *potE* and *puuP* (85, 64, 17, and 6 counts per million transcripts, respectively) for W3110 grown in
119 liquid motility medium (18). We conclude that extracellular putrescine and its transport contribute
120 to PDSM.
121
122 **Putrescine catabolism affected surface motility.**
123 Because putrescine catabolism modulates intracellular putrescine concentrations (19, 20),
124 we examined PDSM in putrescine catabolic mutants. The major putrescine catabolic pathway is
125 initiated with putrescine glutamylation (Figure 6A, right column), and a second pathway initiates
126 with putrescine deamination (Figure 6A, left column) (20). Deletion of either *puuA* or *patA* which
127 code for the first enzymes of their respective pathways did not affect surface motility (Figure 6B).

128 A double mutant moved less well which was unexpected because the proposed higher intracellular
129 putrescine should have stimulated PDSM. Consistent with the stimulatory effect of putrescine, loss
130 of *puuR* which codes for the repressor of PuuA-initiated pathway genes (20), impaired PDSM
131 (Figure 6B). One possible explanation to reconcile these seemingly contradictory results is that an
132 optimal polyamine concentration stimulates PDSM, and a high concentration is inhibitory. The
133 next section describes experiments to test this possibility.
134
135 **High putrescine reduced expression of pili genes.**
136 High putrescine inhibits translation of some mRNAs, and high spermidine, a product of
137 putrescine metabolism, inhibits growth (21, 22). If the phenotype of the Δ*patA* Δ*puuA* double
138 mutant results from spermidine toxicity, then loss of spermidine synthase (SpeE) should reverse
139 the phenotype. This prediction was not met which argues against spermidine toxicity (Figure
140 6C). For the *speB* mutant, 1 mM putrescine stimulated PDSM, and 4 mM putrescine was slightly
141 inhibitory (Figure 7A and B). The concentric ring pattern was observed with 1 mM, but not 4
142 mM putrescine. RT-qPCR to test transcriptional regulation of pili expression by putrescine
143 showed optimal *fimA* transcription at 1 mM putrescine in the *speB* mutant (Figure 7C). Indirect
144 enzyme linked immunosorbent assays (ELISAs) against FimA suggested that the level of FimA
145 in the *speB* mutant at 1 mM putrescine was higher than with 4 mM putrescine, but the difference
146 was not statistically significant (Figure 7D). Variation of supplemental putrescine did not affect
147 FimA in the parental strain (Figure 7C and 7D). Transmission electron microscopy (TEM)
148 showed that pili expression was highest for the *speB* mutant at 1 mM putrescine (Figure 8),
149 moderate at 0.1- and 4-mM putrescine, and undetectable without putrescine. The cells grown
150 with 4 mM putrescine were shorter and thinner, which suggests stress, possibly mimicking

151 osmotic stress. From these results and those in the previous section, we conclude that pili
152 expression required an optimal putrescine concentration.
153
154 **RNAseq analysis identifies *fim* operon expression and energy metabolism as targets of**
155 **putrescine control.**
156 RNAseq analysis was used to further confirm or determine whether putrescine affected
157 (a) transcription of the *fim* operon that codes for the pili structural genes, (b) *fim* operon promoter
158 orientation, i.e. phase variation, or (c) energy metabolism: surface motility of W3110 has been
159 shown to require glucose metabolism and oxidative phosphorylation (10).
160 RNAseq analysis. We grew parental W3110 and its Δ*speB* derivative with and without 1
161 mM putrescine. R^2 values of pairwise comparisons showed that the transcriptome of the *speB*
162 mutant grown without putrescine differed from the other transcriptomes which were similar
163 (Table 1 and Supplemental Figure 2). A multidimensional scaling plot and a plot of the 100 most
164 variable genes visualize these comparisons (Figure 9A and B). When compared to the parental
165 strain, the *speB* mutant grown without putrescine had 310 downregulated genes and 159
166 upregulated genes with at least four-fold differential expression and FDR < 0.05. Transcripts for
167 the putrescine-induced *puuAP* and *puuDRCBE* operons, which specify genes of the major
168 putrescine catabolic pathway, were reduced from 1.6- to 14-fold fold (FDR ≤ 0.02) in the *speB*
169 mutant (Supplemental Table 1). Because higher intracellular putrescine results in higher
170 catabolic gene expression, these results imply lower intracellular putrescine in the Δ*speB* mutant.
171 Transcription of the *fim* operon is reduced in the Δ*speB* mutant. Deletion of *speB* reduced
172 transcripts for genes of the *fimA* operon (Figure 10A). Numerous transcription factors activate
173 the *fim* operon (23, 24), and, of these, loss of *speB* reduced *hns* transcripts, increased *fis*, *lrp*, and

174 *qseB* transcripts, but had no effect on *ihfA* and *ihfB* (Figure 10B). Loss of *hns*, *ihfA*, and *lrp*
175 impaired PDSM (Figure 10C and D), which confirms the requirement for their products for pili
176 synthesis in our strain background.

177 Putrescine does not control *fim* operon phase variation in W3110. The phase ON-favoring
178 FimB and phase OFF-favoring FimE recombinases control the orientation of the *fim* operon
179 promoter. Our version of W3110 has an insertion in *fimE* which means that FimB is the major
180 factor that controls phase variation. Loss of *speB* reduced transcripts from *fimB* which could
181 account for loss of motility. Using specific primers, PCR analysis showed that loss of *speB*, loss
182 of *hns*, or the presence of putrescine did not alter the ratio of ON to OFF (Supplemental Figure
183 3). This experiment determines the steady state phase ON to OFF ratio, which less FimB might
184 not affect if FimB is in excess. In strains with FimE, the rate of phase ON orientation will be
185 much slower and even small changes in FimB activity could conceivably affect the switch
186 orientation. We conclude that putrescine does not control phase variation, at least in our strain of
187 W3110.

188 Evidence for a putrescine homeostatic network. Altered transcript levels in the *speB*
189 mutant suggest compensatory mechanisms for low putrescine (Supplemental Table 1 for
190 transcript differences for all genes, Table 2 for selected genes, and Figure 11 for a diagrammatic
191 representation of transcript differences). The *speB* mutant had more transcripts from (a) genes of
192 arginine and ornithine carboxylase, (b) all genes of ornithine and arginine synthesis from
193 glutamate, and (c) genes for three separate putrescine transport systems; and fewer transcripts
194 from the *sap* operon which codes for a putrescine exporter (25) and *rpmH* and *rpsT*, whose
195 products inhibit ornithine and arginine decarboxylase (26). The net effect of these changes
196 should be to increase intracellular putrescine (solid arrows in Figure 11). In other words, these

197 changes are compensatory for low putrescine. In addition to these changes, the *speB* mutant had
198 60-fold and 7-fold more transcripts for *mgtA* and *phoBR* which code for the major magnesium
199 transporter and the regulators of phosphate assimilation, respectively. These changes may also be
200 compensatory and are discussed below.

201 Putrescine affects energy metabolism which could account for loss of motility. Loss of
202 *speB* affected transcripts for genes of the major energy metabolism pathways (Table 2): fewer
203 transcripts for genes coding for all citric acid cycle enzymes, NADH dehydrogenase I (the entire
204 *nuo* operon), cytochrome oxidase (the *cyo* operon), and several genes of menaquinone (the
205 *menFDHBCE* operon), ubiquinone, and heme synthesis. The *speB* mutant also had fewer
206 transcripts for all genes of iron acquisition, which is consistent with diminished oxidative energy
207 generation. A *speB* mutant had fewer transcripts for *ptsH* (Hpr of the phosphotransferase system
208 of carbohydrate transport), *ptsG* (enzyme IIBC component of glucose transport), *gltA* (citrate
209 synthase), *sdhA* (a succinate dehydrogenase subunit), and *sucC* (a succinyl-CoA synthetase
210 subunit), and their loss has been shown to either impair or eliminate W3110 surface motility
211 (10). The cumulative effect of these differences could account for the motility defect in the *speB*
212 mutant.
213

214 **Discussion**

215 Several aspects of polyamine metabolism affect PDSM in *E. coli*. Strains with loss of one
216 or two polyamine synthesis genes — *speA* and *speB* single mutants and a *speC speF* double mutant
217 — resulted in PDSM defects. This observation is remarkable because nine enzymes and several
218 pathways are involved in polyamine synthesis. Our putrescine synthesis mutants had no growth
219 defect which is not unexpected since deletions of eight biosynthetic genes were required to show

220 a strong phenotype: impaired aerobic growth and elimination of anaerobic growth (3). Strains with
221 defects in the two most active putrescine transport systems had altered PDSM. The specific defects
222 suggest the involvement of extracellular putrescine and arginine in intracellular putrescine
223 homeostasis. The PDSM defect of putrescine transport mutants not only implicates extracellular
224 putrescine but also suggests secretion of putrescine which is not added to the medium. The PDSM
225 defect of *speA* and *speB* mutants implicates extracellular arginine because SpeA is mostly
226 periplasmic (27). Defective putrescine catabolism also affected PDSM. The role of both putrescine
227 synthesis and degradation suggests rapid adjustments to fluctuating putrescine concentrations and
228 environmental conditions: putrescine catabolism is a core response to several stresses (19).

229 Results from an RNAseq analysis showed that transcription of the *fim* operon was reduced
230 in the *speB* mutant. Of the known transcription factors that control the *fim* operon, only the gene
231 for H-NS had fewer transcripts. In contrast, transcripts for other relevant transcription factor genes
232 were elevated in the *speB* mutant. Our results are consistent with H-NS mediating putrescine-
233 dependent control, but we cannot exclude a general regulatory dysfunction mediated by altered
234 nucleoprotein complexes at the *fim* operon promoter. The elevated transcripts for some
235 transcription factors may be inhibitory.

236 The transcriptomic results showed that the *speB* mutant had more transcripts for genes
237 whose products will maintain intracellular putrescine, which suggests compensatory mechanisms
238 for low intracellular putrescine (Figure 11). The *speB* mutant also had more transcripts for
239 magnesium and phosphate transport genes. The elevated transcripts for magnesium transport
240 genes could compensate for low putrescine to the extent that magnesium can directly replace
241 putrescine, e.g., binding to nucleotides and RNA (28). Two recent studies observe an inverse
242 correlation between intracellular magnesium and polyamines in *Salmonella* and proposed that

243 either magnesium or the polyamines maintained an overall divalent cation homeostasis (29, 30).
244 The rationale for an increase in anionic phosphate assimilation is less clear, although the major
245 phosphate permease transports metal-phosphates, including magnesium-phosphate (31), which
246 could help to compensate for low putrescine. Regardless of the rationale, the substantial changes
247 in gene expression due to low putrescine suggest multiple compensatory mechanisms.

248 A major observation of the RNAseq analysis is that loss of *speB* lowered transcripts for
249 many genes of energy metabolism and all genes of iron acquisition. This gene expression pattern
250 suggests that low putrescine diverts metabolism away from energy generation and toward
251 putrescine synthesis, i.e., a prioritization of putrescine synthesis over aerobic energy metabolism.
252 Oxidative energy metabolism and putrescine synthesis compete for α-ketoglutarate and the
253 metabolic diversion could also be a potential compensatory mechanism for low putrescine.
254 Another way of looking at this relationship is that intracellular putrescine positively correlates
255 with oxidative energy metabolism. Deletion of *ptsH*, *ptsG*, *gltA*, *sdhA*, and *sucC* have been
256 shown to impair W3110 PDSM which suggests that a major, possibly the primary, effect of low
257 putrescine is reduced energy generation.

258 In contrast to our results, a thorough and well-designed study showed that *E. coli* PDSM
259 requires spermidine instead of putrescine (8). The differences between the studies were strain
260 backgrounds, media (glucose-LB vs glucose-tryptone), and incubation temperature (33º vs 37º).
261 We found PDSM results for 37º incubations were highly variable and resulted in numerous fast-
262 moving variants. Since growth at the higher temperature is faster, and faster growth is associated
263 with higher putrescine (32), we propose that growth at 37º results in an inhibitory putrescine
264 concentration. In this case, spermidine would be stimulatory because of its known inhibition of the
265 putrescine biosynthetic enzymes SpeA and SpeC (33, 34) and subsequent reduction of intracellular

266 putrescine to an optimal concentration. Regardless of the explanation, strains differences are not
267 unexpected because of decades of strain passage for the strains employed with resulting laboratory
268 evolution that can affect any of the numerous factors that control the intracellular putrescine
269 concentration.

270 The transcript changes observed in our study were different from those in the only other
271 systematic study of putrescine's effect on *E. coli* gene expression (6). Both studies had almost
272 identical experimental designs: 1.0- or 1.14-mM putrescine was added to a *speB* or *speB speC*
273 mutant, respectively. Differences in strains, growth media (minimal media vs tryptone-containing
274 media), and growth temperature (33° vs 37°) could account for the discrepancy in results. The most
275 crucial difference could be the growth media: Igarashi and colleagues grew bacteria in a minimal
276 medium, while we grew bacteria in an amino acid-containing medium that was required for surface
277 motility. We propose that the slower growth in minimal medium, possibly correlated with higher
278 guanosine tetraphosphate which is associated with slower growth, counters and obscures many
279 growth-stimulatory putrescine effects. In contrast, the growth stimulation from the amino acids in
280 our medium would not counter putrescine effects and would essentially allow detection of effects
281 caused solely by changes in putrescine concentrations. Regardless of the explanation, common
282 results can be interpreted as core responses to putrescine limitation. Both studies observed that low
283 putrescine increased transcripts for genes of arginine synthesis and magnesium transport, and
284 reduced transcripts for the *sdhCDAB-sucABCD* operon which codes for three TCA cycle enzymes.
285 The link between putrescine and arginine synthesis is probably mediated by the ArgR repressor
286 because *argR* transcripts are 2.5-fold lower (FDR = 0.0004) in the *speB* mutant (Supplemental
287 Table 1).

288 Several results implicate putrescine in *E. coli* virulence during urinary tract infections.
289 First, pili-dependent binding to the urothelium is an essential step for uropathogenic *E. coli* (35).
290 Second, putrescine is present in urine from infected, but not healthy, individuals (36, 37). Third,
291 urinary putrescine can result from uropathogenic *E. coli* growth in urine (37) and urothelial
292 pathophysiology (38). Putrescine's possible role in virulence is seemingly contradicted by the
293 observation that a *speB* mutant outcompetes the parental CFT073 in the bladder of mice, i.e., less
294 putrescine synthesis enhanced virulence (39). A majority of uropathogenic *E. coli* are associated
295 with phylogenetic group B2—including CFT073, whereas most *E. coli* lab strains, such as W3110,
296 are group A. Group B2 strains lack genes for the major putrescine catabolic pathway and have
297 significantly higher transcripts for genes coding for SpeA and SpeB (18). Both observations
298 suggest that the cytoplasmic putrescine concentration is higher in group B2 strains. We propose
299 that the putrescine concentration in group B2 strains is normally in the inhibitory range for pili
300 synthesis, and that loss of SpeB reduces putrescine to a level that stimulates pili synthesis.
301 Regardless of the explanation, putrescine control of pili synthesis and other processes in
302 uropathogenic *E. coli* are worth examination.
303
304

305 ## Experimental Procedures

306 **Strains.** All strains used for growth rate determinations and motility assays were derivatives of *E.*
307 *coli* K-12 strain W3110 and are listed in Table 3. Great variations exist in standard lab strains,
308 including W3110, from different labs. We initially tested nine strains derived from *E. coli* K-12,
309 mostly from the Coli Genetic Stock Center (9), and chose our lab strain because of relative genetic
310 stability and more quantitatively reproducible results. Our strain originated from the lab of Jon

311 Beckwith in the 1960s via the lab of Boris Magasanik where it had been stored in a room
312 temperature stab until the mid-1980s, at which time it was revived and frozen at -80º C. To
313 construct the mutant strains, the altered allele was obtained from the Keio collection in which the
314 gene of interest had been deleted and replaced with an antibiotic resistance gene (40). The marked
315 deletion allele was transferred into W3110 by P1 transduction (41). The antibiotic gene was
316 removed as described which generated an in-frame deletion (42).
317
318 **Media and Growth Conditions.** For P1 transductions and plasmid transformation experiments,
319 cells were grown in standard LB liquid medium (1% tryptone, 1% NaCl and 0.5% yeast extract,
320 pH 7.0) at 37°C. Antibiotics were used for selection at concentrations of 25 μg/mL (both
321 chloramphenicol and kanamycin). For growth analysis, bacteria were grown in liquid motility
322 medium (0.5% glucose, 1% tryptone, and 0.25% NaCl) which we refer to as GT medium. Starter
323 cultures (typically 6–12 h incubation) were grown in GT medium, harvested by centrifugation,
324 washed twice with phosphate buffered saline and re-suspended in GT medium before inoculation.
325 The cells were then grown at 37° C in aerobic conditions (shaking at 240 rpm) and the turbidity
326 was measured every thirty minutes. Cell growth was measured in Klett units using a Scienceware
327 Klett colorimeter with a KS-54 filter. 100 Klett units represent an OD_{600} value of about 0.7.
328
329 **Surface motility assay.** For a standard surface motility assay, single colonies from fresh plates
330 (streaked out from frozen stocks a day before) were inoculated in GT medium for six hours at
331 37° C in aerobic conditions (shaking at 240 rpm). 30 ml of autoclaved GT medium with 0.45%
332 agar (Eiken, Tokyo, Japan) was poured into sterile polystyrene petri-dish (100 mm X 15 mm)
333 and allowed to solidify at room temperature for approximately six hours. Then, 1 μL of the pre-

334 motility growth medium was inoculated at the center of the agar plate and incubated at 33° C for
335 36 hrs. Each experiment was performed in triplicate and pictures were taken after 36 hours.
336 Surface motility was extremely sensitive to humidity. Opening the incubator before 36 hours
337 resulted in movement cessation. The surface motility assay was performed at 33º C because
338 results from incubations at 37º C were highly variable and the cultures more frequently generated
339 genetically stable fast-moving variants.
340
341 **Swim assay.** The media and culturing for swimming motility is identical to that for surface
342 motility, except that the plates contained 0.25% agar and were solidified at room temperature for
343 about one hour before inoculation. Then, 1 μL of the culture was stabbed in the center of this
344 swim agar plate and incubated at 33° C for 20 hours. Each experiment was performed in
345 triplicate.
346
347 **Transmission electron microscopy.** Cells from surface motility plates were collected and fixed
348 with 2.5% glutaraldehyde. Bacteria were absorbed onto Foamvar carbon-coated copper grids for
349 1 min. Grids were washed with distilled water and stained with 1% phosphotungstic acid for 30
350 s. Washed and stained grids were dried at 37ºC for 10 minutes. Samples were viewed on a JEOL
351 1200 EX transmission electron microscope at University of Texas Southwestern Medical Center
352 (Figure 2) and University of Texas at Dallas (Figure 8).
353
354 **ELISA analysis.** Cells were grown overnight in 5 mL GT media followed by a 2-hour growth in
355 GT media with 0.0, 0.1, 1.0, or 4.0 mM putrescine. Cells were then lysed using a 24-gauge
356 needle. The cell lysate was diluted to a concentration of 1 mg/mL protein (based on A280) in pH

357 9.6 coating buffer (3 g Na_2CO_3, 6 g $NaHCO_3$, 1000 mL distilled water) and then coated onto the
358 walls of a 96-well plate by incubating overnight at 4°C. The wells were rinsed 3 times with PBS
359 and further blocked using coating buffer with 1% bovine albumin overnight at 4°C. The
360 following day, wells were rinsed 3 times with PBS, and primary antibodies to FimA or RpoD
361 were added following supplier directions. After a 2-hour room temperature incubation, secondary
362 antibodies conjugated to HRP were added and incubated for a further two hours. HRP was
363 activated using the TMB substrate kit (Thermo-34021) following the provided protocol.
364 Expression was read on a BioTek plate reader based on the provided kit protocol. Data was
365 blanked to wells only treated with bovine albumin then normalized to RpoD. Data was generated
366 from technical and biological triplicates.
367
368 **DNA isolation and genome assembly and annotation for W3110.** DNA was isolated based on
369 previous established protocols (43). Short reads were sequenced at the SeqCenter (Pittsburgh,
370 Pennsylvania) using Illumina tagmentation-based and PCR-based DNA prep and custom IDT
371 indices targeting inserts of 280 bp without further fragmentation or size selection steps. The
372 Illumina NovaSeq X Plus sequencer was ran producing 2X151 paired-end reads.
373 Demultiplexing, quality control, and adapter trimmer was performed with bcl-convert (v4.2.4).
374 Total Illumina Reads (R1+R2): 4059078 with 553087045 bps >Q30.
375 Long reads were prepared using the PCR-free Oxford Nanopore Technologies ligation
376 sequencing kit with the NEBNext companion module. No fragmentation or size selection was
377 performed. Long read libraries were performed using R10.4.1 flow cell. The 400bps sequencing
378 mode with a minimum read length of 200bp were selected. Gupply (v6.5.7) was used at the

379 super-accurate basecalling, demultiplexing, and adapter removal. Total long reads: 53773 with
380 89.607 % of bps > Q20.
381 To generate the completed genome, porechop (v0.2.4) was used to trim residual adapter
382 sequences from long reads. Flye (v2.9.2) was used to generate the *de novo* assembly under the
383 nano-hq model. Reads longer than the estimated N_{50} based on a genome size of 6Mbp initiated
384 the assembly. Subsequent polishing using the short read data was performed using Pilon (v1.24)
385 under default parameters. Long read contigs with an average short read coverage of 15X or less
386 were removed from the assembly. The assembled contig was confirmed to be circular via
387 circulator (v1.5.5). Annotation was performed using prokka (v 1.14.6). Finally, statistics were
388 recorded using QUAST (v5.2.0). The final genome contained 1 contig of 4750347 bp with a
389 sequencing depth of 123.92x. The N_{50} was 4750347. This genome can be accessed via the
390 accession number CP165600 or via the BioProject PRJNA1142534 via NCBI. The completed
391 genome has an estimated average nucleotide identity of 99.9694 to the W3110 genome deposited
392 to NCBI (genome assembly ASM1024v1).
393
394 **RNA isolation and quality control.** Cells were grown for 2 hours in 1 mL GT media. 60 µL
395 were then added to 1 mL of fresh GT, with or without 1 mM putrescine, and grown for another
396 two hours. After growth, the cells were centrifuged, and frozen at -80ºC. The isolation and
397 analysis protocol has been previously published (18). Cell pellets were thawed, resuspended in
398 0.7 mL of buffer RLT (Qiagen RNeasy kit), and mechanically lysed using a bead beater
399 (FastPrep-24 Classic from MP Biomedical) set at the highest setting for three 45-s cycles with a
400 5-min rest period on ice between cycles. Cell lysates were used to isolate RNA using a Qiagen
401 RNeasy mini kit. RNA was quantified, DNase treated, and re-quantified on a nanodrop. RNA

402 that passed the first quality check was analyzed on RNA-IQ (Qubit). RNA with an IQ higher
403 than 7.5 was used. RNA that passed both checks were run on an agarose gel to check for RNA
404 integrity. RT-qPCR was used to ensure there was no DNA contamination. RNA libraries that
405 passed all these quality checks were submitted to the genomics core facility at The University of
406 Texas at Dallas for RNA sequencing. The core performed rRNA removal (RiboMinus
407 Transcriptome Isolation Kit or RiboCop bacterial rRNA depletion—Lexogen), library
408 preparation (Stranded Total RNA Prep—Illumina), and single-end Illumina sequencing.
409
410 **Reverse transcription quantitative PCR.** RNA was isolated as described above. One
411 microgram of RNA was reverse transcribed using LunaScript RT Super Mix (NEB E3010) and
412 another microgram was subjected to the same reaction as the reverse transcribed RNA, except
413 without reverse transcriptase (negative control) following manufacturer instructions. The cDNA
414 was then diluted to 10 ng/µL for qPCR. PCR reactions were composed of 10 ng cDNA, 8 µL of
415 nuclease free water, 10 nM primers (rpoD: Forward: TCGTGTTGAAGCAGAAGAAGCG;
416 Reverse: TCGTCATCGCCATCTTCTTCG) (fimA: Forward: ATGGTGGGACCGTTCACTTT;
417 Reverse: GGCAACAGCGGCTTTAGATG), and PowerUp SYBR Green 2X master mix for
418 qPCR (ThermoFisher A25777) in a 20 µL reaction. A Quantstudio 3 qPCR machine was used to
419 generate critical threshold (Ct) values. The Ct values were then analyzed using the $2^{-\Delta\Delta C_T}$ method
420 (44) using *rpoD* as a library control.
421
422 **RNAseq Analysis.** Transcripts were aligned to the W3110 genome and CDS (CP165600)
423 available on NCBI using CLC genomics workbench (Qiagen version 22.00) for RNA-seq
424 analysis. The gene expression counts generated as this output were used to perform differentially

425 expressed gene (DEG) analysis using EdgeR (version 3.38.4) to analyze read counts (45, 46).
426 DEGs had an adjusted P-value less than 0.05.
427
428 **Data availability:** The raw RNA seq reads were deposited in GenBank: BioProject accession
429 number PRJNA1126736. The genome was deposited in GenBank: BioProject accession number
430 PRJNA1142534. The genome accession number is CP165600.
431
432 **Acknowledgements:** This work was funded through private donations. PEZ received
433 endowment support from the Cain Foundation through the Felecia and John Cain Distinguished
434 Chair in Women's Health in honor of Philippe E. Zimmern, MD. The authors declare no potential
435 conflicts of interests.
436 The authors (JH, SH, GV, and LR) would like to thank Prof. Kelli Palmer of The
437 University of Texas at Dallas for the use of her space, supplies, and tissue homogenizer. JH
438 would like to further thank Prof. Palmer for the use of her CLC genomics program. The authors
439 would like to thank the Genome Center at The University of Texas at Dallas for the services to
440 support our research. The authors would like to thank the Olympus Discovery Center/Imaging
441 Core facility at UT Dallas for providing equipment and support (Figure 8), and the UT
442 Southwestern Medical Center for electron microscopy (Figure 2).
443
444
445 **References:**

446 1. Tabor CW, Tabor H. 1984. Polyamines. Annual review of biochemistry 53:749-90.
447 2. Tabor CW, Tabor H. 1984. Polyamines. Annu Rev Biochem 53:749-90.

448 3. Chattopadhyay MK, Tabor CW, Tabor H. 2009. Polyamines are not required for aerobic growth of
449 *Escherichia coli*: preparation of a strain with deletions in all of the genes for polyamine
450 biosynthesis. J Bacteriol 191:5549-52.
451 4. Igarashi K, Kashiwagi K. 2000. Polyamines: mysterious modulators of cellular functions. Biochem
452 Biophys Res Commun 271:559-64.
453 5. Igarashi K, Kashiwagi K. 2015. Modulation of protein synthesis by polyamines. IUBMB Life
454 67:160-9.
455 6. Yoshida M, Kashiwagi K, Shigemasa A, Taniguchi S, Yamamoto K, Makinoshima H, Ishihama A,
456 Igarashi K. 2004. A unifying model for the role of polyamines in bacterial cell growth, the
457 polyamine modulon. J Biol Chem 279:46008-13.
458 7. Armbruster CE, Hodges SA, Mobley HL. 2013. Initiation of swarming motility by *Proteus mirabilis*
459 occurs in response to specific cues present in urine and requires excess L-glutamine. J Bacteriol
460 195:1305-19.
461 8. Kurihara S, Suzuki H, Tsuboi Y, Benno Y. 2009. Dependence of swarming in *Escherichia coli* K-12
462 on spermidine and the spermidine importer. FEMS Microbiol Lett 294:97-101.
463 9. Ambagaspitiye S, Sudarshan S, Hogins J, McDill P, De Nisco NJ, Zimmern PE, Reitzer L. 2019.
464 Fimbriae and flagella mediated surface motility and the effect of glucose on nonpathogenic and
465 uropathogenic *Escherichia coli* BioRxiv doi.org:10.1101/840991
466 10. Sudarshan S, Hogins J, Ambagaspitiye S, Zimmern P, Reitzer L. 2021. The nutrient and energy
467 pathway requirements for surface motility of nonpathogenic and uropathogenic *Escherichia coli*.
468 J Bacteriol. doi:10.1128/jb.00467-20doi:10.1128/jb.00467-20.
469 11. Yokota T, Gots JS. 1970. Requirement of adenosine 3', 5'-cyclic phosphate for flagella formation
470 in *Escherichia* coli and *Salmonella typhimurium*. J Bacteriol 103:513-6.
471 12. Conway C, Beckett MC, Dorman CJ. 2023. The DNA relaxation-dependent OFF-to-ON biasing of
472 the type 1 fimbrial genetic switch requires the Fis nucleoid-associated protein. Microbiology
473 (Reading). 169(1):doi:10.1099/mic.0.001283.
474 13. Kelly A, Conway C, T OC, Smith SG, Dorman CJ. 2006. DNA supercoiling and the Lrp protein
475 determine the directionality of fim switch DNA inversion in *Escherichia coli* K-12. J Bacteriol
476 188:5356-63.
477 14. O'Gara JP, Dorman CJ. 2000. Effects of local transcription and H-NS on inversion of the fim switch
478 of *Escherichia coli*. Mol Microbiol 36:457-66.
479 15. Tabor CW, Tabor H. 1985. Polyamines in microorganisms. Microbiol Rev 49:81-99.
480 16. Igarashi K, Ito K, Kashiwagi K. 2001. Polyamine uptake systems in *Escherichia coli*. Res Microbiol
481 152:271-8.
482 17. Kurihara S, Suzuki H, Oshida M, Benno Y. 2011. A novel putrescine importer required for type 1
483 pili-driven surface motility induced by extracellular putrescine in *Escherichia coli* K-12. J Biol
484 Chem 286:10185-92.
485 18. Hogins J, Xuan Z, Zimmern PE, Reitzer L. 2023. The distinct transcriptome of virulence-associated
486 phylogenetic group B2 *Escherichia coli*. Microbiol Spectr. doi:10.1128/spectrum.02085-
487 23e0208523. doi:10.1128/spectrum.02085-23.
488 19. Schneider BL, Hernandez VJ, Reitzer L. 2013. Putrescine catabolism is a metabolic response to
489 several stresses in *Escherichia coli*. Mol Microbiol 88:537-50.
490 20. Schneider BL, Reitzer L. 2012. Pathway and enzyme redundancy in putrescine catabolism in
491 *Escherichia coli*. J Bacteriol 194:4080-8.
492 21. Fukuchi J, Kashiwagi K, Yamagishi M, Ishihama A, Igarashi K. 1995. Decrease in cell viability due
493 to the accumulation of spermidine in spermidine acetyltransferase-deficient mutant of
494 *Escherichia coli*. J Biol Chem 270:18831-5.

22. Sakamoto A, Sahara J, Kawai G, Yamamoto K, Ishihama A, Uemura T, Igarashi K, Kashiwagi K, Terui Y. 2020. Cytotoxic mechanism of excess polyamines functions through translational repression of specific proteins encoded by polyamine modulon. Int J Mol Sci. 21(7):doi:10.3390/ijms21072406.
23. Schwan WR. 2011. Regulation of *fim* genes in uropathogenic *Escherichia coli*. World J Clin Infect Dis 1:17-25.
24. Karp PD, Ong WK, Paley S, Billington R, Caspi R, Fulcher C, Kothari A, Krummenacker M, Latendresse M, Midford PE, Subhraveti P, Gama-Castro S, Muniz-Rascado L, Bonavides-Martinez C, Santos-Zavaleta A, Mackie A, Collado-Vides J, Keseler IM, Paulsen I. 2018. The EcoCyc Database. EcoSal Plus. 8(1):doi:10.1128/ecosalplus.ESP-0006-2018.
25. Sugiyama Y, Nakamura A, Matsumoto M, Kanbe A, Sakanaka M, Higashi K, Igarashi K, Katayama T, Suzuki H, Kurihara S. 2016. A novel putrescine exporter SapBCDF of *Escherichia coli*. J Biol Chem 291:26343-26351.
26. Keseler IM, Mackie A, Santos-Zavaleta A, Billington R, Bonavides-Martínez C, Caspi R, Fulcher C, Gama-Castro S, Kothari A, Krummenacker M, Latendresse M, Muñiz-Rascado L, Ong Q, Paley S, Peralta-Gil M, Subhraveti P, Velázquez-Ramírez DA, Weaver D, Collado-Vides J, Paulsen I, Karp PD. 2016. The EcoCyc database: reflecting new knowledge about *Escherichia coli* K-12. Nucleic Acids Research 45:D543-D550.
27. Tabor H, Tabor CW. 1969. Partial separation of two pools of arginine in *Escherichia coli*; preferential use of exogenous rather than endogenous arginine for the biosynthesis of 1,4-diaminobutane. J Biol Chem 244:6383-7.
28. Miyamoto S, Kashiwagi K, Ito K, Watanabe S, Igarashi K. 1993. Estimation of polyamine distribution and polyamine stimulation of protein synthesis in *Escherichia coli*. Arch Biochem Biophys 300:63-8.
29. Iwadate Y, Golubeva YA, Slauch JM. 2023. Cation homeostasis: Coordinate regulation of polyamine and magnesium levels in *Salmonella*. mBio 14:e0269822.
30. Duprey A, Groisman EA. 2020. DNA supercoiling differences in bacteria result from disparate DNA gyrase activation by polyamines. PLoS Genet 16:e1009085.
31. van Veen HW, Abee T, Kortstee GJ, Konings WN, Zehnder AJ. 1994. Translocation of metal phosphate via the phosphate inorganic transport system of *Escherichia coli*. Biochemistry 33:1766-70.
32. Tweeddale H, Notley-McRobb L, Ferenci T. 1998. Effect of slow growth on metabolism of *Escherichia coli*, as revealed by global metabolite pool ("metabolome") analysis. J Bacteriol 180:5109-16.
33. Applebaum DM, Dunlap JC, Morris DR. 1977. Comparison of the biosynthetic and biodegradative ornithine decarboxylases of *Escherichia coli*. Biochemistry 16:1580-4.
34. Wu WH, Morris DR. 1973. Biosynthetic arginine decarboxylase from *Escherichia coli*. Purification and properties. J Biol Chem 248:1687-95.
35. Flores-Mireles AL, Walker JN, Caparon M, Hultgren SJ. 2015. Urinary tract infections: epidemiology, mechanisms of infection and treatment options. Nat Rev Microbiol 13:269-84.
36. Puebla-Barragan S, Renaud J, Sumarah M, Reid G. 2020. Malodorous biogenic amines in *Escherichia coli*-caused urinary tract infections in women-a metabolomics approach. Sci Rep 10:9703.
37. Satink HP, Hessels J, Kingma AW, van den Berg GA, Muskiet FA, Halie MR. 1989. Microbial influences on urinary polyamine excretion. Clin Chim Acta 179:305-14.
38. Keay SK, Birder LA, Chai TC. 2014. Evidence for bladder urothelial pathophysiology in functional bladder disorders. Biomed Res Int 2014:865463.

39. Alteri CJ, Smith SN, Mobley HL. 2009. Fitness of *Escherichia coli* during urinary tract infection requires gluconeogenesis and the TCA cycle. PLoS Pathog 5:e1000448.
40. Baba T, Ara T, Hasegawa M, Takai Y, Okumura Y, Baba M, Datsenko KA, Tomita M, Wanner BL, Mori H. 2006. Construction of *Escherichia coli* K-12 in-frame, single-gene knockout mutants: the Keio collection. Mol Syst Biol 2:2006 0008.
41. Miller JH. 1972. Experiments in Molecular Genetics. Cold Spring Harbor Laboratory, Cold Spring Harbor, NY.
42. Datsenko KA, Wanner BL. 2000. One-step inactivation of chromosomal genes in *Escherichia coli* K-12 using PCR products. Proc Natl Acad Sci U S A 97:6640-5.
43. Hogins J, Zimmern PE, Reitzer L. 2023. Genome sequences of seven clade B2 *Escherichia coli* strains associated with recurrent urinary tract infections in postmenopausal women. Microbiol Resour Announc doi:10.1128/mra.00035-23:e0003523.
44. Livak KJ, Schmittgen TD. 2001. Analysis of relative gene expression data using real-time quantitative PCR and the 2(-Delta Delta C(T)) Method. Methods 25:402-8.
45. McCarthy DJ, Chen Y, Smyth GK. 2012. Differential expression analysis of multifactor RNA-Seq experiments with respect to biological variation. Nucleic Acids Res 40:4288-97.
46. Robinson MD, McCarthy DJ, Smyth GK. 2010. edgeR: a Bioconductor package for differential expression analysis of digital gene expression data. Bioinformatics 26:139-40.

Table 1. Pairwise statistical comparisons of transcriptomes. Abbreviation: putr is putrescine

Strain 1	**Strain 2**	R^2
Wild-type (1 mM putr)	wild-type (0 mM putr)	0.950
Wild-type (1 mM putr)	Δ*speB* (1 mM putr)	0.954
Δ*speB* (0 mM putr)	Δ*speB* (1 mM putr)	0.820
Δ*speB* (0 mM putr)	wild-type (0 mM putr)	0.796
Δ*speB* (0 mM putr)	wild-type (1 mM putr)	0.786

Table 2. Differentially expressed genes that are proposed to contribute to putrescine homeostasis. A positive number means more transcripts in the Δ*speB* (lower putrescine) strain.

Gene (function)	log_2FC	FDR
Polyamine synthesis		
speA (putrescine)	0.99	0.003
speC (putrescine)	1.43	3E-4
speD (spermidine)	-0.83	0.01
speF (putrescine)	1.05	0.007
rpmH (inhibitor of SpeA and SpeC)	-2.77	2E-4
rpsT (inhibitor of SpeA and SpeC)	-1.92	8E-4
Polyamine transport		
*potABCD** (spermidine)	-2.17	3E-4
potE (putrescine)	2.07	2E-4
*potFGHI** (putrescine)	1.41	4E-4
plaP (putrescine)	1.11	0.005
*sapBCDF** (putrescine export)	-1.18	8E-4
Arginine synthesis		
argA_2 (synthesis)	1.77	0.001
argB (synthesis)	1.87	0.002
argC (synthesis)	2.86	0.005
argD (synthesis)	1.41	0.001
argF (synthesis)	1.63	0.01
argG (synthesis)	2.32	0.002
argH (synthesis)	0.97	0.001
argI (synthesis)	1.95	0.018
argR (repressor of arginine regulon)	-1.35	4E-4
Glutamate generation		
glsA (glutamine degradation)	2.16	5E-4

glnG (regulation of ammonia assimilation)	-1.59	0.022
TCA cycle/electron transport		
acnA (TCA cycle)	-1.04	8E-4
acnB (TCA cycle)	-1.96	2E-4
fumA (TCA cycle)	-1.50	6E-4
fumB (TCA cycle)	-1.49	0.003
gltA (TCA cycle)	-1.64	2E-4
icdA (TCA cycle)	-1.32	0.002
*sdhCDAB-sucABCD** (TCA cycle)	-3.88	5E-5
nuo operon* (electron transport)	-0.82	0.004
*menFDHBCE** (electron transport)	-0.8	0.005
*ubiEJB** (electron transport)	-0.93	0.004
*cyoABCD** (electron transport)	-1.41	9E-4
*hemCD** (heme)	-2.05	2E-4
Iron transport		
*exbBD** (transport of all iron chelates)	-2.33	4E-5
tonB (transport of all iron chelates)	-1.9	4E-5
*entCEBA** (enterochelin iron)	-5.2	7E-6
fecABCDE * (ferric citrate)	-4.4	3E-5
fecIR (regulators, ferric citrate)	-4.4	6E-6
*feoABC** (ferrous iron)	-3.4	7E-4
fur (regulator, iron assimilation)	-0.40	0.11
Magnesium and phosphate transport		
mgtA (magnesium)	5.90	5E-6
phoQ (regulator, magnesium)	0.79	0.009
*pstSCAB** (phosphate)	3.61	0.01

*phoBR** (regulator, phosphate assimilation)	2.80	0.02

570

571 * Values for transcripts of the first gene of operon are given. Results for other genes of the

572 operon are in Supplemental Table 1

573

574

575 Table 3. Strains

Strain Name	Genotype	Reference
BLS77	W3110 Δ*puuR*::*cat*	(20)
BLS80	W3110 Δ*puuA*::*cat*	(20)
BLS88	W3110 Δ*patA* Δ*puuA*	(20)
CP2	W3110 Δ*patA*	(20)
IM26	W3110 Δ*speB::kan fliC-lacZ*	This study
IM27	W3110 Δ*speE::kan fliC-lacZ*	This study
IM28	W3110 Δ*speF::cat fliC-lacZ*	This study
IM29	W3110 Δ*speC::kan fliC-lacZ*	This study
IM34	W3110 Δ*speC* Δ*speF::cat fliC-lacZ*	This study
IM60	W3110 Δ*cadA::kan fliC-lacZ*	This study
IM61	W3110 Δ*speA::kan*	This study
IM62	W3110 Δ*patA* Δ*puuA* Δ*speE::kan*	This study
IM63	W3110 Δ*potE::kan*	This study
IM64	W3110 Δ*potF::kan*	This study
IM65	W3110 Δ*plaP::kan*	This study
IM66	W3110 Δ*puuP::kan*	This study
J15	W3110 Δ*speB* Δ*fliC*::*kan*	This study
SA1	W3110 Δ*fliC::kan*	This study
SA2	W3110 Δ*fimA::kan*	This study
SA3	W3110 Δ*fliC* Δ*fimA*	This study

SA4	W3110 Δ*hns::kan*	This study
SA5	W3110 Δ*ihfA::kan*	This study
SA6	W3110 Δ*lrp::kan*	This study
W3110-LR referred to as W3110	*lacI*^{q} *lacL8*	Lab strain

576 **Figure legends:**

577 Figure 1 Pathways and enzymes of polyamine synthesis.

578

579 Figure 2. Surface motility of W3110. (A) Surface motility of parental and derivative strains lacking
580 the major subunits of the flagella (FliC), pili (FimA), or both. (B) TEM images of cells of W3110
581 and W3110 Δ*fliC* Δ*fimA* taken from the movement's edge directly from surface motility plates.
582 (C) Swimming motility with and without 0.5% glucose.

583

584 Figure 3. Genetics of surface motility. (A) PDSM of mutants with defects in polyamine anabolic
585 genes. All assays were performed in triplicate, and representative images are shown. (B)
586 Diameter of surface movement of polyamine mutants after 36 hours. Error bars represent
587 standard deviations for three independent replicates. Statistical analysis was performed using the
588 Dunnett test of significance: *, $P<0.05$; **, $P<0.01$; ***, $P<0.001$. In this figure the Δ*speB*
589 mutant was IM26.

590

591 Figure 4: Nutritional supplementation of Δ*speB* mutant. (A) Putrescine and spermidine
592 supplementation of wild type and Δ*speB* strains. (B) Diameter of surface movement of

593 polyamine mutants after 36 hours. Error bars represent standard deviations for three independent
594 replicates. Statistical analysis was performed using the Sadik test of significance: *, $P<0.05$; **,
595 $P<0.01$; ***, $P<0.001$. All assays were performed in triplicates and representative images are
596 shown. In this figure the Δ*speB* mutant was IM26.
597
598 Figure 5: Putrescine transport and surface motility. (A) Representative images of surface motility
599 for strains defective in putrescine transport genes. (B) Diameter of surface movement of
600 polyamine mutants after 36 hours. Error bars represent standard deviations for three independent
601 replicates. Statistical analysis was performed using the Dunnett test of significance: *, $P<0.05$;
602 **, $P<0.01$; ***, $P<0.001$. All assays were performed in triplicate and representative images are
603 shown.
604
605 Figure 6: Putrescine catabolism and surface motility. (A) Pathways and enzymes of putrescine
606 catabolism. (B) Motility diameter of putrescine catabolic mutants after 36 hours. Error bars
607 represent standard deviations for three independent replicates. Statistical analysis was performed
608 using the Dunnett test of significance: *, $P<0.05$; **, $P<0.01$; ***, $P<0.001$. All assays were
609 performed in triplicates and representative images are shown. (C) Effect of loss of *speE* on the
610 *patA puuA* catabolic double mutant.
611
612 Figure 7: Surface motility and pili expression in W3110 and Δ*speB*. (A) W3110 Δ*speB* surface
613 motility with 0.0, 0.1, 1.0, and 4.0 mM exogenous putrescine. All assays were performed in
614 triplicate. Representative images are shown. (B) Average diameter of 3 separate surface motility
615 plates. The parental strain without putrescine is shown for reference. Significance was

616 determined by comparing the diameters of the Δ*speB* mutants in the different concentrations of
617 putrescine compared to the parental W3110. One way ANOVA was used with Dunnett
618 hypothesis testing to determine p values, ***, $p < 0.001$. (C) Reverse transcriptase-quantitative
619 PCR using primers targeting the *fimA* gene from cells grown in 0.0, 0.1, 1.0, and 4.0 mM of
620 supplemented putrescine. Double deltas were generated by normalizing the parental and the
621 Δ*speB* mutant RNA libraries to *rpoD* then comparing *fimA* expression. Two-way ANOVA was
622 used to determine significance followed by Sadik hypothesis testing. ***, $p<0.001$. (D) Enzyme
623 linked immunosorbent assays using antibodies targeting pili (FimA) from cells grown with 0.0,
624 0.1, 1.0, and 4.0 mM of supplemented putrescine. Two-way ANOVA was used to determine
625 significance followed by FDR adjusting. ***, $p<0.001$. In this figure the Δ*speB* mutant was J15.
626
627 Figure 8: Transmission electron micrographs of Δ*speB* mutant cells after surface motility.
628 Representative images are shown and cells were removed from motility plates with the following
629 exogenous putrescine concentrations: (A) none, (B) 0.1 mM, (C) 1.0 mM, and (D) 4.0 mM. No
630 pili were observed with 0 and 0.1 mM putrescine. Optimal pili production was observed with 1.0
631 mM putrescine. The bar represents one micron. In this figure the Δ*speB* mutant was J15.
632
633 Figure 9: Visual representation of the results from transcriptomic sequencing of W3110 and the
634 Δ*speB* mutant's gene expression in media with and without 1.0 mM putrescine. (A)
635 Multidimensional scaling plot of the parental and Δ*speB* mutant transcriptomes. When grown
636 with 1.0 mM putrescine (red), the Δ*speB* mutant transcriptome (triangles) are nearly identical to
637 the parental transcriptomes when grown without and with putrescine (blue and red circles,
638 respectively). When grown without putrescine, the Δ*speB* mutant transcriptome (blue triangles)

639 is greatly skewed from transcriptomes of the parental strain and the Δ*speB* mutant grown with
640 putrescine. (B) Heatmap of the top 100 most variable genes further demonstrates the
641 distinctiveness of the Δ*speB* mutant grown without putrescine and the similarities of the Δ*speB*
642 mutant transcriptome when grown with 1.0 mM putrescine supplementation and the parental
643 grown with or without putrescine. In this figure the Δ*speB* mutant was J15.
644
645 Figure 10: Transcriptomic sequencing of genes for the *fim* region and regulators that control *fim*
646 gene expression. (A) Expression of the *fim* genes in the parental W3110 and the *speB* mutant
647 with and without putrescine supplementation. Values were calculated by dividing the individual
648 replicates' counts per million (CPM) value for each gene by the mean CPM of that gene in
649 W3110 grown without putrescine and multiplying by 100 to yield the percent expression. Arrows
650 below the genes signify the known operons: *fimB* and *fimE* belong to single gene operons, while
651 *fimAICDFGH* belong to one operon. One way ANOVA was used to determine significance using
652 Dunnett hypothesis testing. **, $p < 0.01$; ***, $p < 0.001$. (B) Expression of some regulators
653 known to affect *fim* gene expression. Values were calculated as described in (A). ***, $p < 0.001$.
654 (C) Surface motility of W3110 and three regulator mutants (Δ*hns*, Δ*ihfA*, and Δ*lrp*). A gene
655 found to be significantly different by this transcriptomic analysis (*hns*) was confirmed to be
656 important in surface motility. In this figure the Δ*speB* mutant was J15. (D) Diameter of surface
657 movement of regulatory mutants after 36 hours. Error bars represent standard deviations for three
658 independent replicates. Statistical analysis was performed using the Dunnett test of significance:
659 *, $P<0.05$; **, $P<0.01$; ***, $P<0.001$. All assays were performed in triplicate.
660
661

662

663 Figure 11: The deduced diversion of metabolism in a *speB* mutant away from energy metabolism
664 toward putrescine synthesis compared to the parental strain. The effects of low putrescine are
665 shown. Genes and processes (transport and transcriptional regulators) in red have fewer
666 transcripts, while those in black or blue have more. The dashed lines represent proposed
667 reduction in metabolic flux because of fewer transcripts from genes coding for the enzymes
668 involved. Operons are shown except for the larger operons or regulons. For example, *pur* is
669 meant to represent the unlinked genes that code for enzymes of purine synthesis. Table 2 or
670 Supplemental Table 1 should be consulted for specific genes and the quantitative change in
671 transcripts.

672

673 Supplemental Figure 1: Growth and swimming of polyamine anabolic mutants.

674

675 Supplemental Table 1. Differential gene expression analysis of W3110 and Δ*speB*. J15 refers to
676 the Δ*speB* mutant. In the tab labeled "W3110_0_vs_J15_1_ Putrescine" W3110 was grown
677 without putrescine, J15 was grown with 1.0 mM putrescine; positive fold change values refer to
678 increases in J15 gene expression.

679

680 Supplementary Figure 2. Expression graphs comparing the logCPM of the transcriptomes of the
681 average of the three replicates of W3110 with and without 1 mM putrescine and the *speB*
682 mutant with and without 1 mM putrescine. A regression line was calculated and the correlation
683 between each set of transcriptomes noted on the graph. Higher R^2 values indicate greater
684 similarity between the transcriptomes.

685

686 Supplemental Figure 3. Phase variation in parental W3110, W3110 Δ*speB*, W3110 Δ*hns*, and

687 MG1655

688

Figure 1

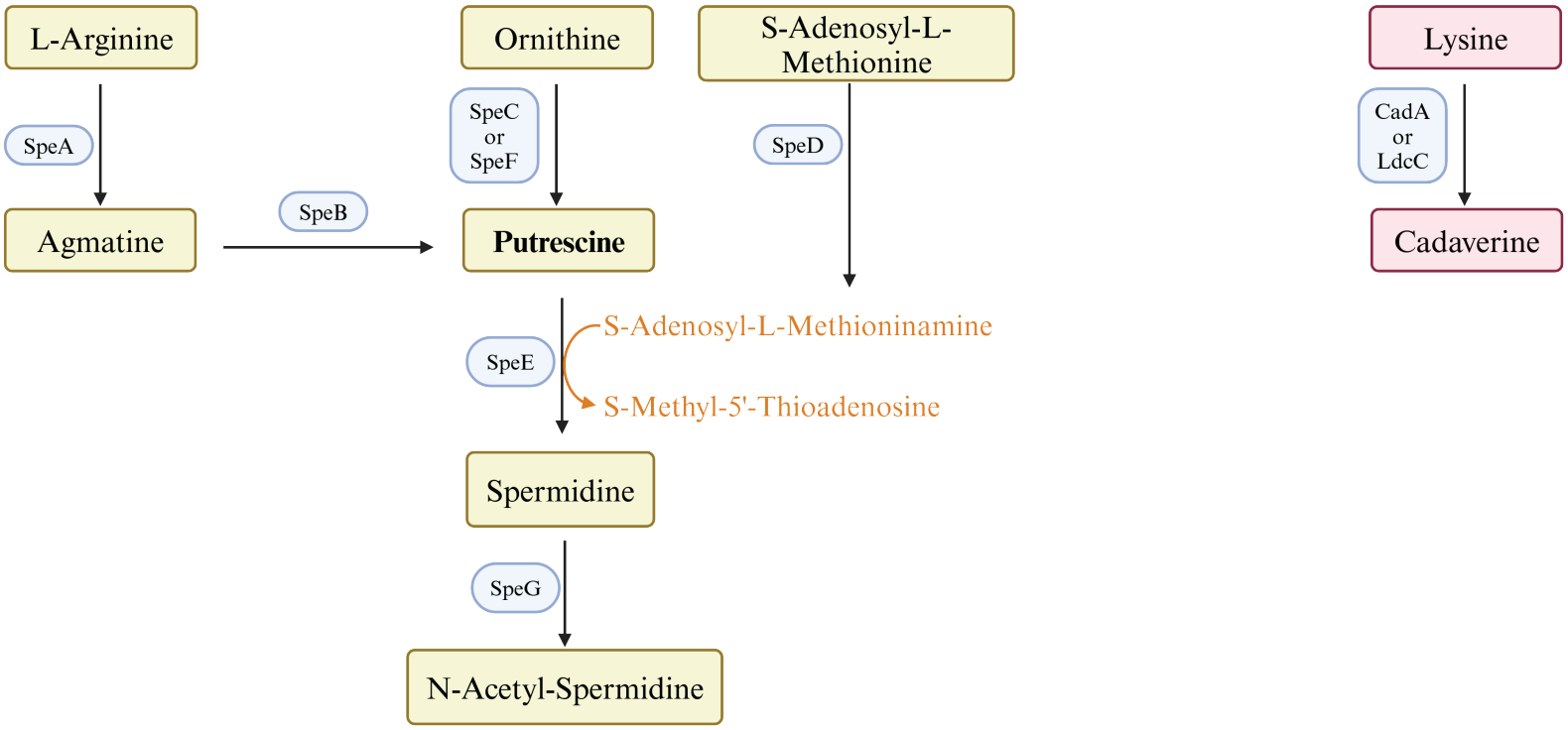

Figure 1 Pathways and enzymes of polyamine synthesis.

Figure 2

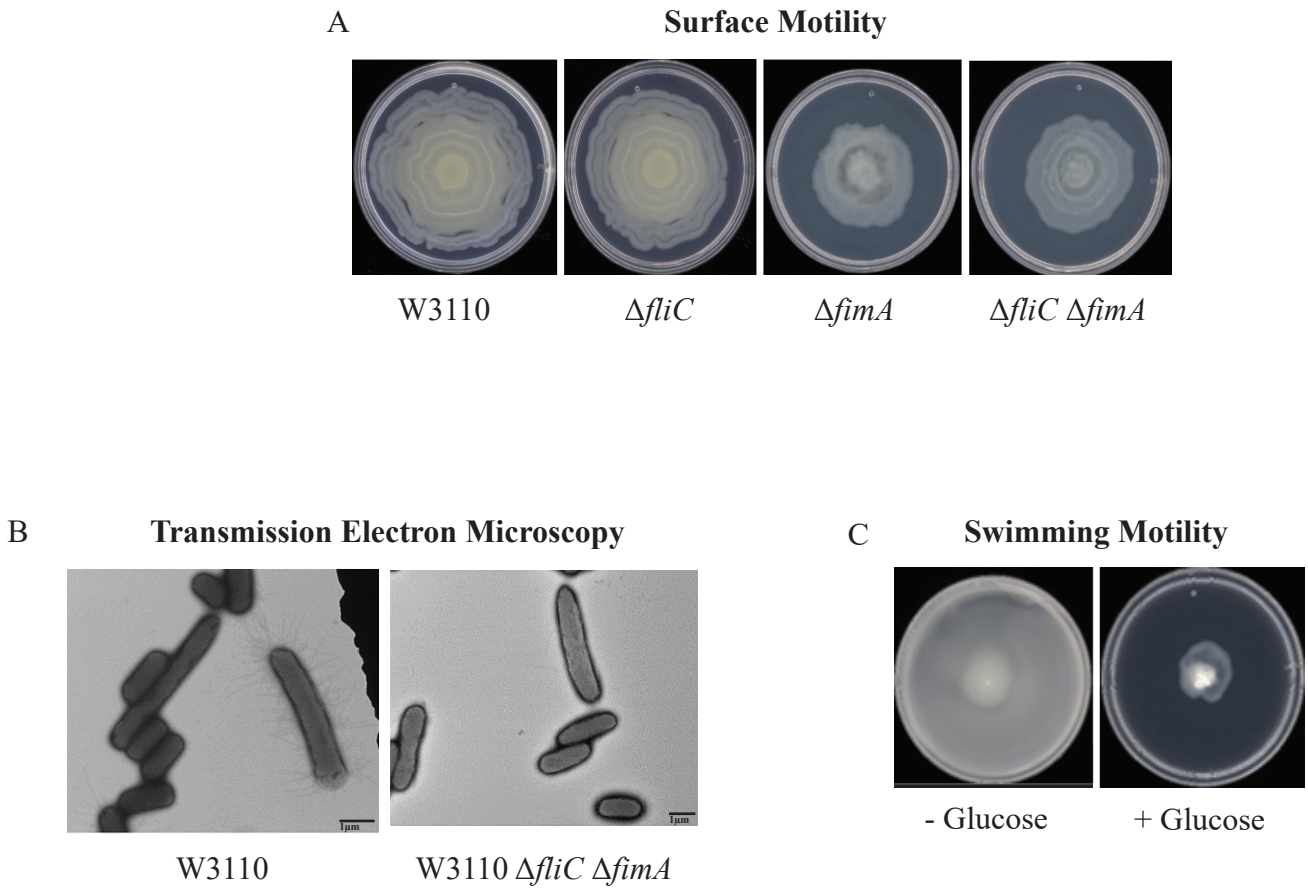

Figure 2. Surface motility of W3110. (A) Surface motility of parental and derivative strains lacking the major subunits of the flagella (FliC), pili (FimA), or both. (B) TEM images of cells of W3110 and W3110 Δ*fliC* Δ*fimA* taken from the movement's edge directly from surface motility plates. (C) Swimming motility with and without 0.5% glucose.

Figure 3

A

Surface Motility of Polyamine Biosynthesis Mutants

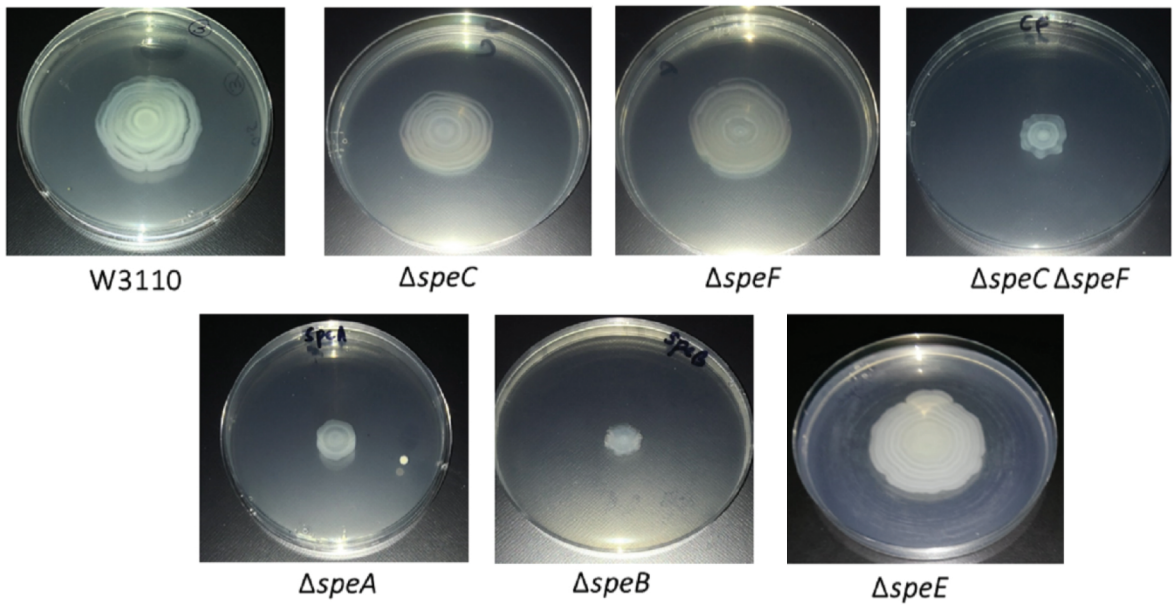

B

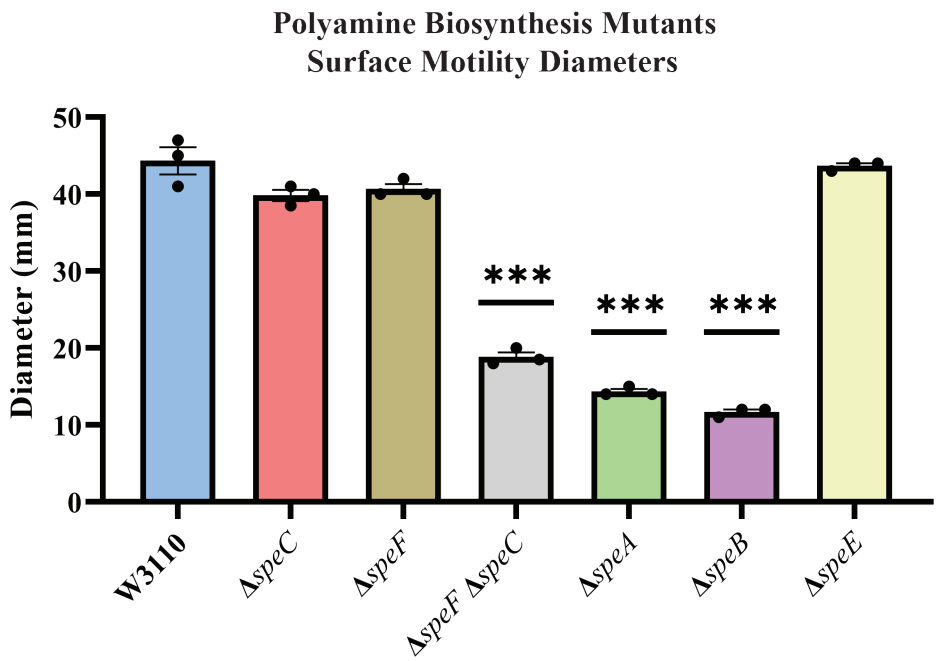

Figure 3 Legend

Figure 3. Genetics of surface motility. (A) PDSM of mutants with defects in polyamine anabolic genes. All assays were performed in triplicate, and representative images are shown. (B) Diameter of surface movement of polyamine mutants after 36 hours. Error bars represent standard deviations for three independent replicates. Statistical analysis was performed using the Dunnett test of significance: *, $P<0.05$; **, $P<0.01$; ***, $P<0.001$. In this figure the Δ*speB* mutant was IM26.

Figure 4

A

Surface Motility with Putrescine and Spermidine Supplementation

No Exogenous Putrescine | 1.0 mM Putrescine | 1.0mM Spermidine

W3110

Δ*speB*

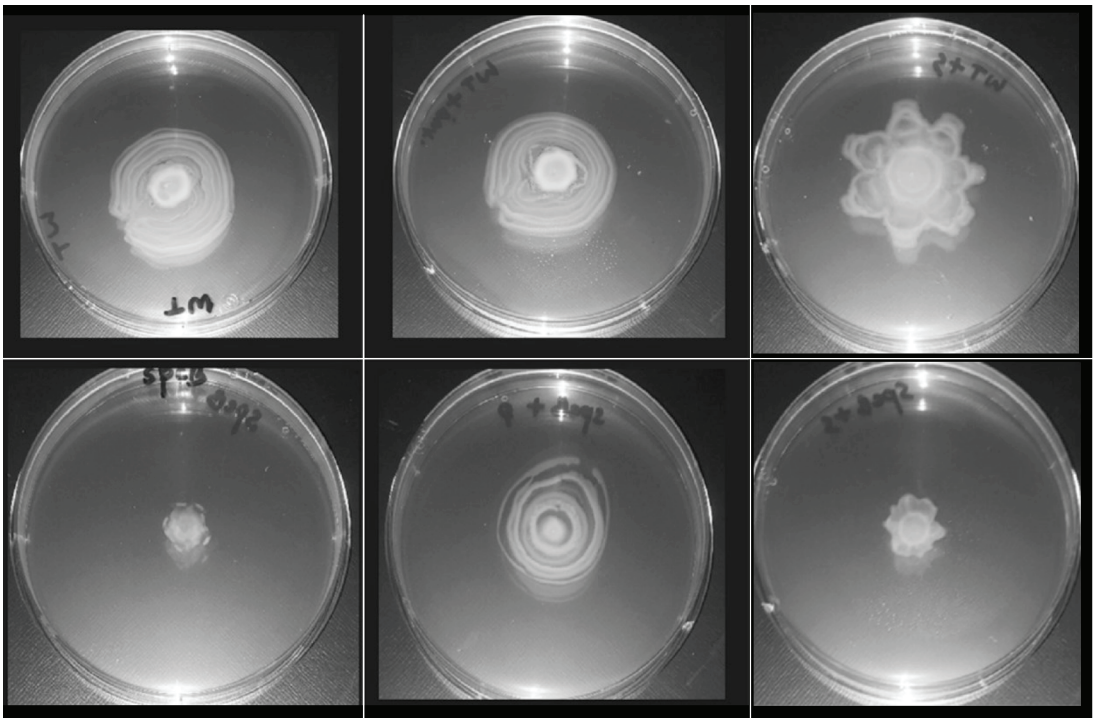

B

Putrescine and Spermidine Supplementation
Surface Motility Diameters

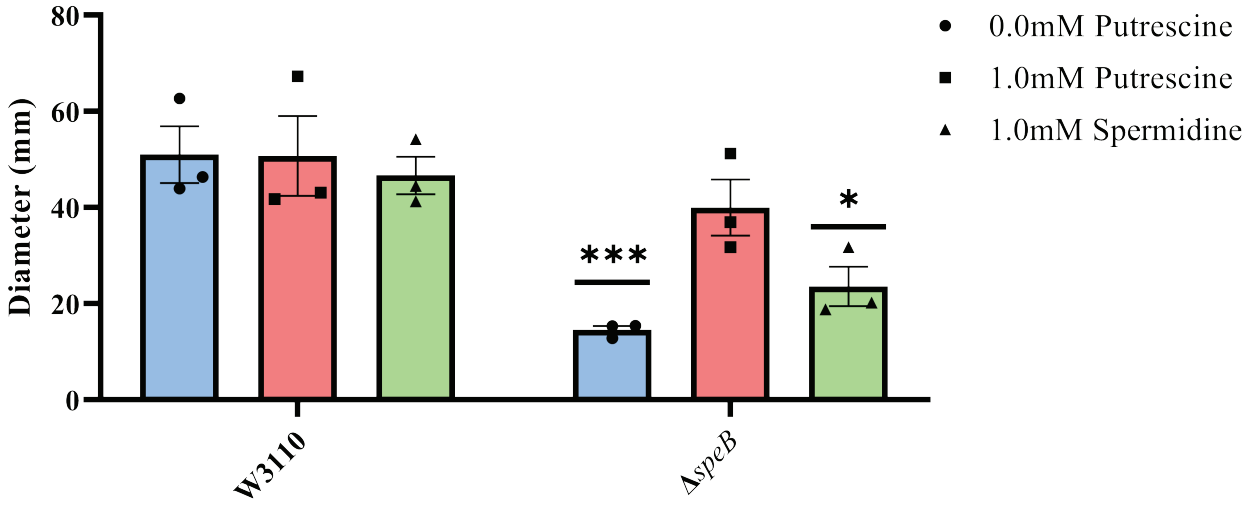

Figure 4 Legend

Figure 4: Nutritional supplementation of Δ*speB* mutant. (A) Putrescine and spermidine supplementation of wild type and Δ*speB* strains. (B) Diameter of surface movement of polyamine mutants after 36 hours. Error bars represent standard deviations for three independent replicates. Statistical analysis was performed using the Sadik test of significance: *, $P<0.05$; **, $P<0.01$; ***, $P<0.001$. All assays were performed in triplicates and representative images are shown. In this figure the Δ*speB* mutant was IM26.

Figure 5

A

Surface Motility of Putrescine Export Mutants

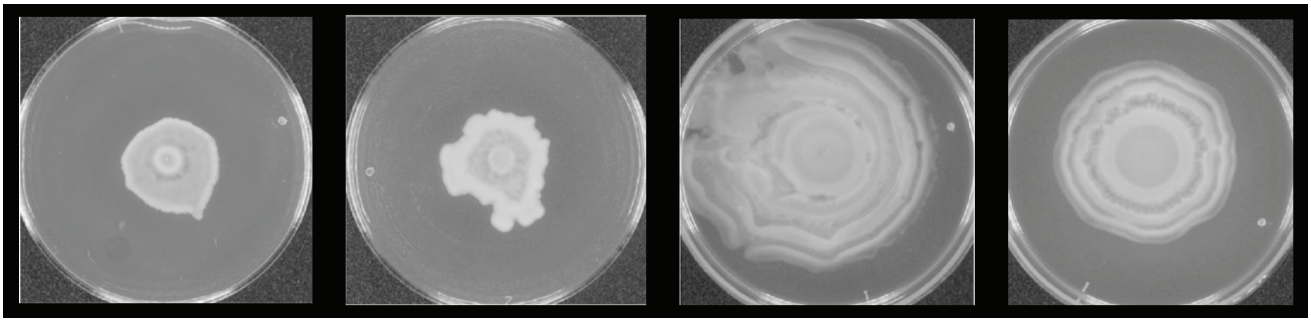

ΔplaP *ΔpotF* *ΔpotE* *ΔpuuP*

B

Putrescine Export Mutant
Surface Motility Diameters

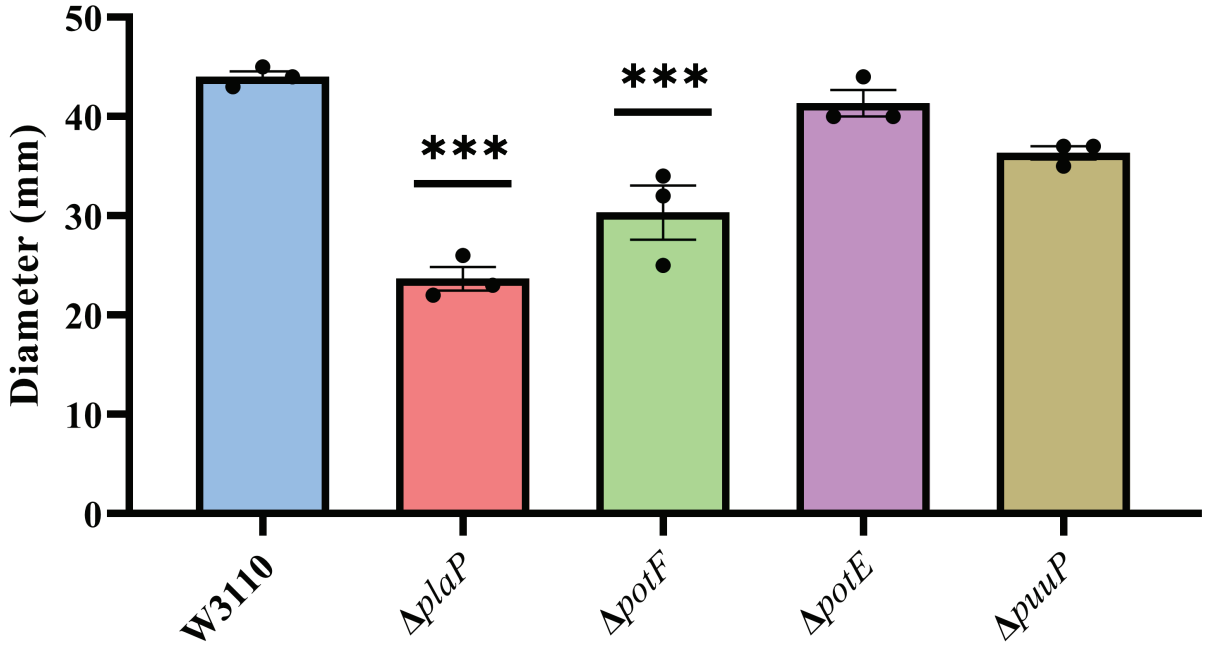

Figure 5: Putrescine transport and surface motility. (A) Representative images of surface motility for strains defective in putrescine transport genes. (B) Diameter of surface movement of polyamine mutants after 36 hours. Error bars represent standard deviations for three independent replicates. Statistical analysis was performed using the Dunnett test of significance: *, P<0.05; **, P<0.01; ***, P<0.001. All assays were performed in triplicate and representative images are shown.

Figure 6

A

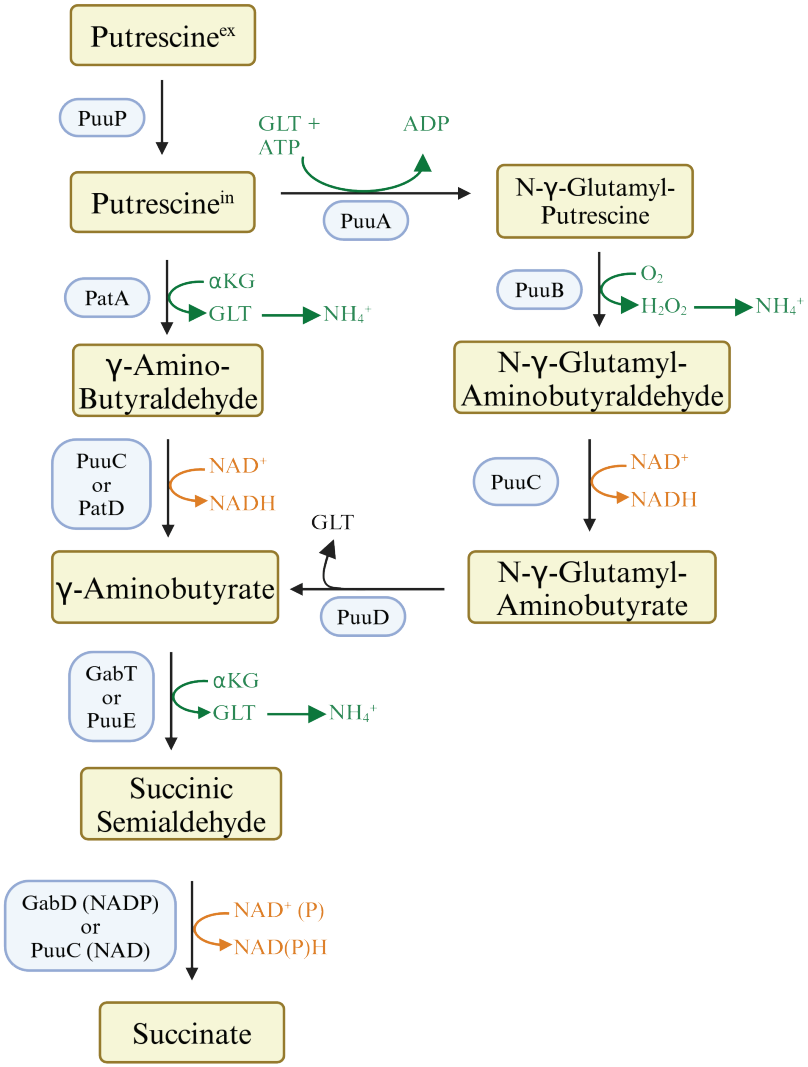
Putrescine^ex
PuuP
Putrescine^in
GLT + ATP
ADP
PuuA
N-γ-Glutamyl-Putrescine
PatA
αKG
GLT
NH4+
PuuB
O2
H2O2
NH4+
γ-Amino-Butyraldehyde
N-γ-Glutamyl-Aminobutyraldehyde
PuuC or PatD
NAD+
NADH
PuuC
NAD+
NADH
GLT
γ-Aminobutyrate
PuuD
N-γ-Glutamyl-Aminobutyrate
GabT or PuuE
αKG
GLT
NH4+
Succinic Semialdehyde
GabD (NADP) or PuuC (NAD)
NAD+ (P)
NAD(P)H
Succinate

B

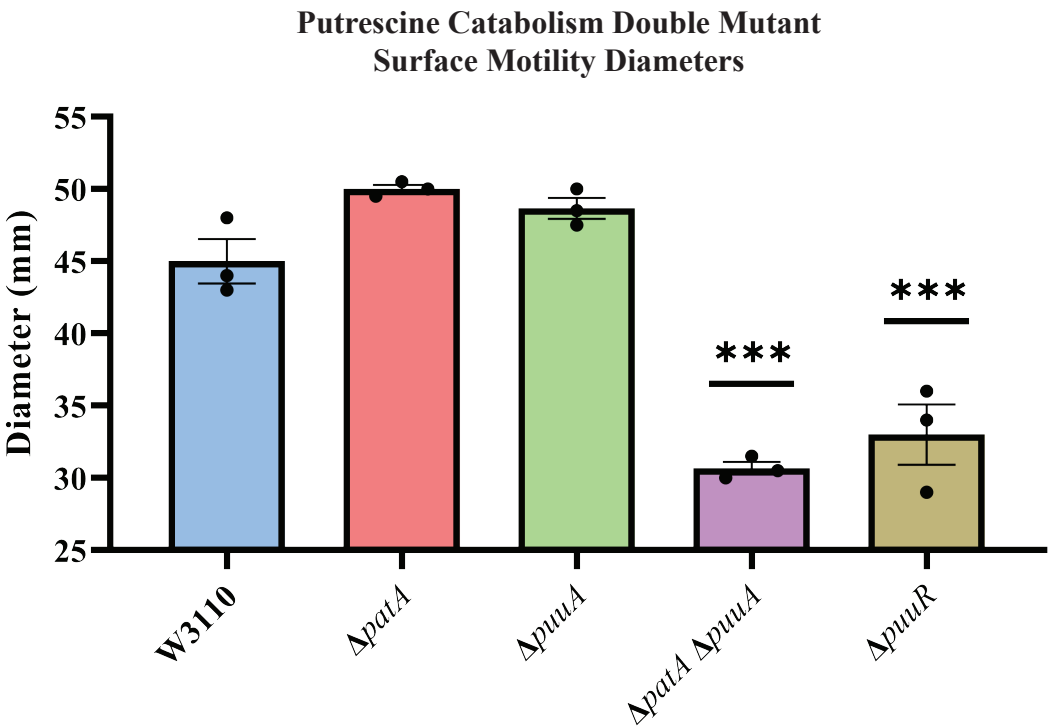
Putrescine Catabolism Double Mutant
Surface Motility Diameters
Diameter (mm)
55
50
45
40
35
30
25
***
***
W3110
ΔpatA
ΔpuuA
ΔpatA ΔpuuA
ΔpuuR

C

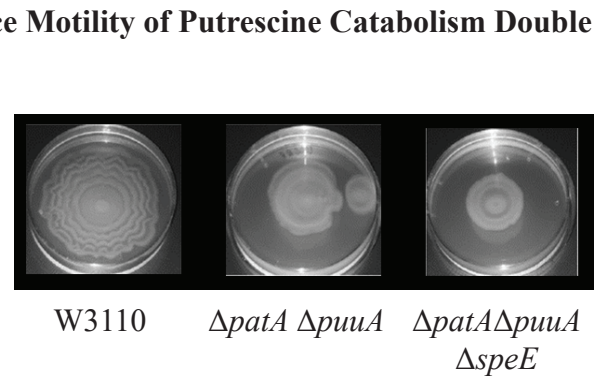
Surface Motility of Putrescine Catabolism Double Mutants
W3110
ΔpatA ΔpuuA
ΔpatAΔpuuA ΔspeE

Figure 6 Legend

Figure 6: Putrescine catabolism and surface motility. (A) Pathways and enzymes of putrescine catabolism. (B) Motility diameter of putrescine catabolic mutants after 36 hours. Error bars represent standard deviations for three independent replicates. Statistical analysis was performed using the Dunnett test of significance: *, $P<0.05$; **, $P<0.01$; ***, $P<0.001$. All assays were performed in triplicates and representative images are shown. (C) Effect of loss of *speE* on the *patA puuA* catabolic double mutant.

Figure 7

A

Surface Motility of the W3110 Δ*speB* Δ*fliC* With and Without Putrescine Supplementation

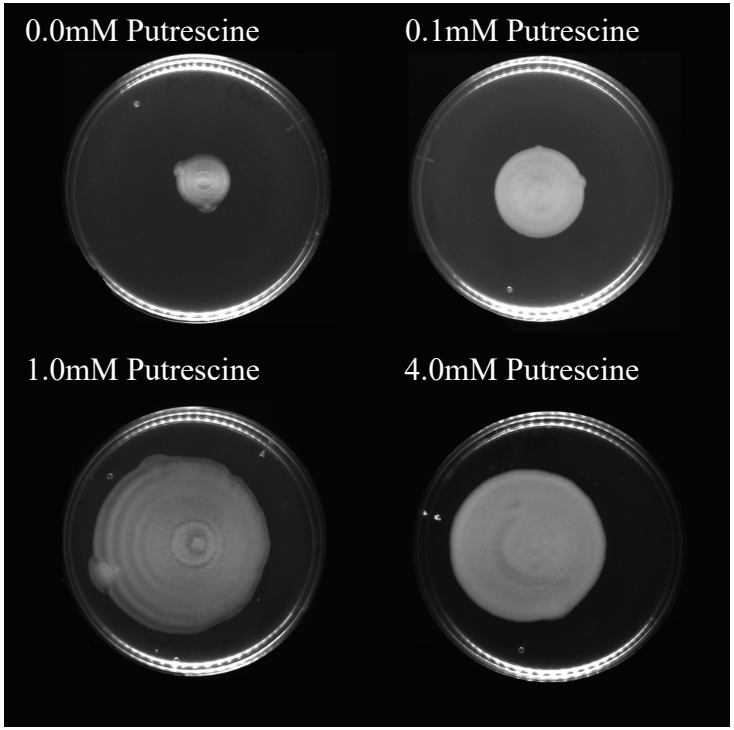

B

W3110 Δ*speB* Δ*fliC* With and Without Putrescine Supplementation Surface Motility Diameters

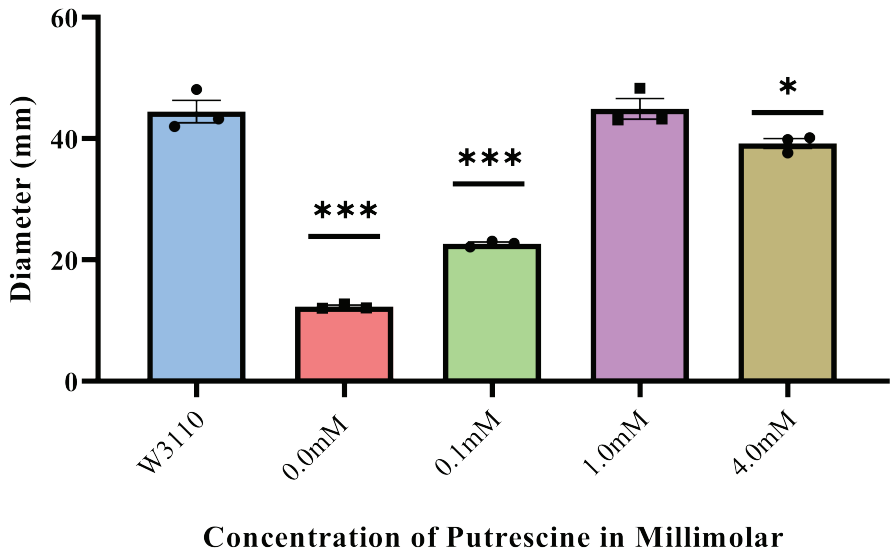

C

RT-qPCR of *fimA*

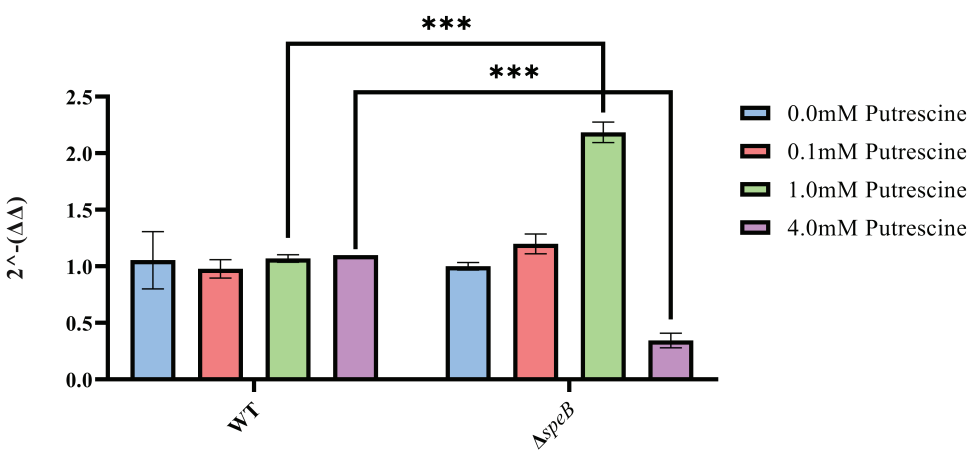

D

ELISA of FimA

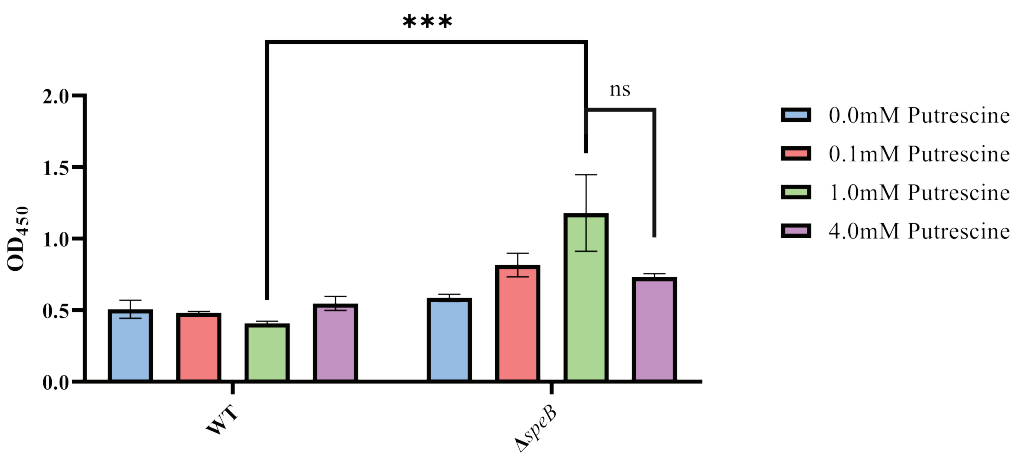

Figure 7 Legend

Figure 7: Surface motility and pili expression in W3110 and ΔspeB. (A) W3110 Δ*speB* surface motility with 0.0, 0.1, 1.0, and 4.0 mM exogenous putrescine. All assays were performed in triplicate. Representative images are shown. (B) Average diameter of 3 separate surface motility plates. The parental strain without putrescine is shown for reference. Significance was determined by comparing the diameters of the Δ*speB* mutants in the different concentrations of putrescine compared to the parental W3110. One way ANOVA was used with Dunnett hypothesis testing to determine p values, ***, $p < 0.001$. (C) Reverse transcriptase-quantitative PCR using primers targeting the *fimA* gene from cells grown in 0.0, 0.1, 1.0, and 4.0 mM of supplemented putrescine. Double deltas were generated by normalizing the parental and the Δ*speB* mutant RNA libraries to *rpoD* then comparing *fimA* expression. Two-way ANOVA was used to determine significance followed by Sadik hypothesis testing. ***, $p<0.001$. (D) Enzyme linked immunosorbent assays using antibodies targeting pili (FimA) from cells grown with 0.0, 0.1, 1.0, and 4.0 mM of supplemented putrescine. Two-way ANOVA was used to determine significance followed by FDR adjusting. ***, $p<0.001$. In this figure the Δ*speB* mutant was J15.

Figure 8

Transmission Electron Microscopy of W3110Δ*speB*
with and without Putrescine Supplementation

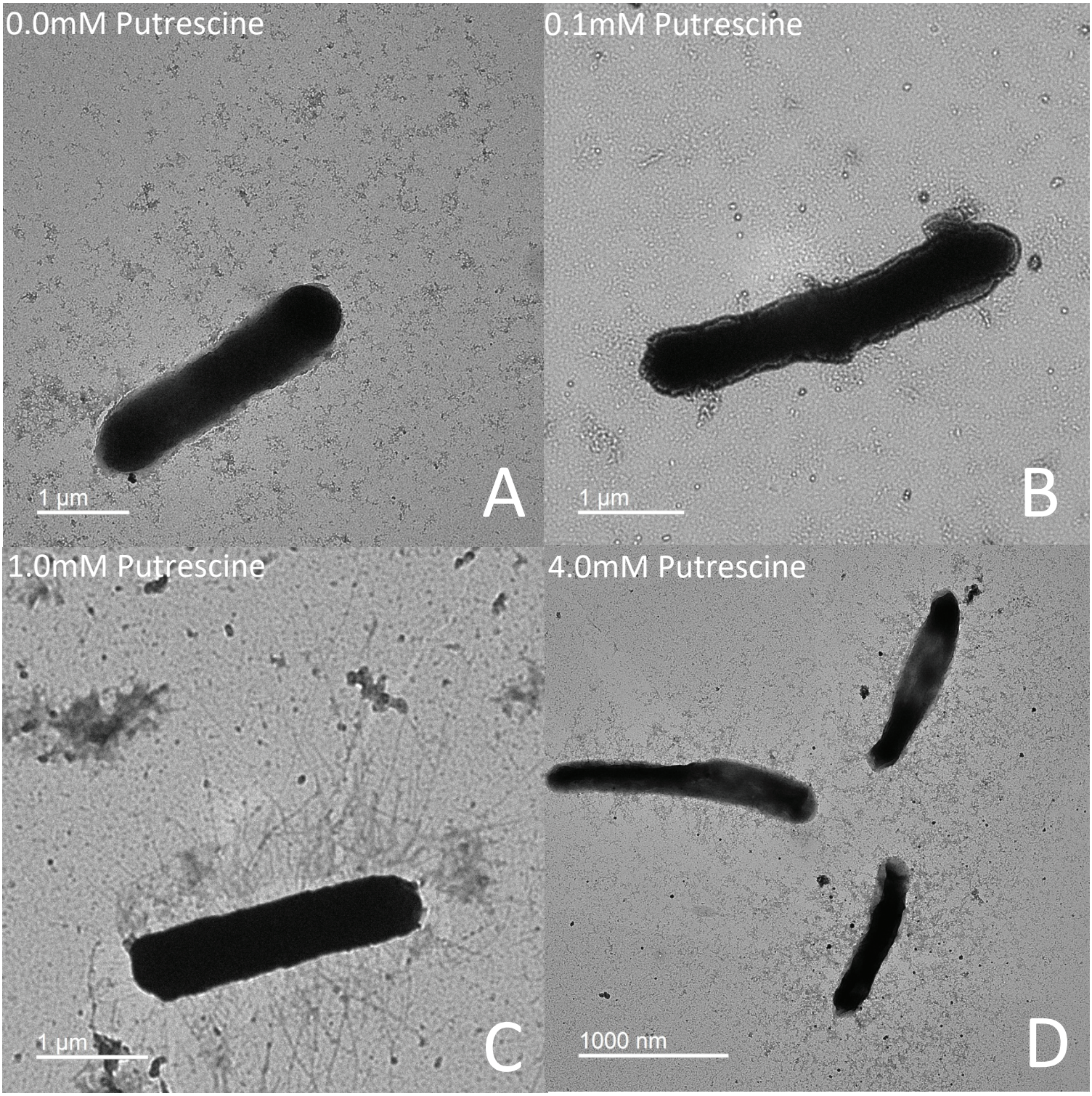

Figure 8 Legend

Figure 8: Transmission electron micrographs of Δ*speB* mutant cells after surface motility. Representative images are shown and cells were removed from motility plates with the following exogenous putrescine concentrations: (A) none, (B) 0.1 mM, (C) 1.0 mM, and (D) 4.0 mM. No pili were observed with 0 and 0.1 mM putrescine. Optimal pili production was observed with 1.0 mM putrescine. The bar represents one micron. In this figure the Δ*speB* mutant was J15.

A

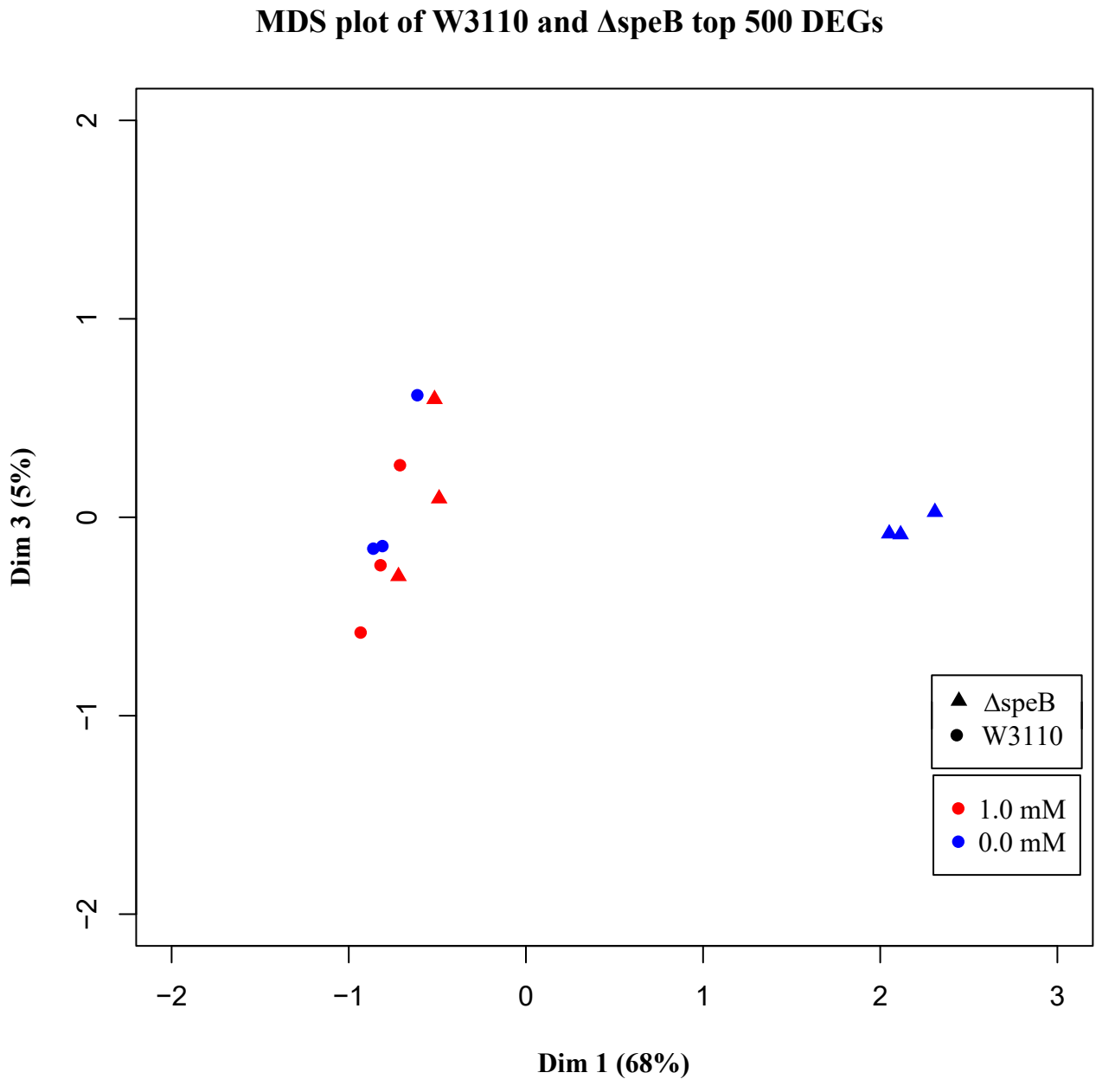
MDS plot of W3110 and ΔspeB top 500 DEGs
Dim 3 (5%)
Dim 1 (68%)
2
1
0
−1
−2
−2
−1
0
1
2
3
ΔspeB
W3110
1.0 mM
0.0 mM

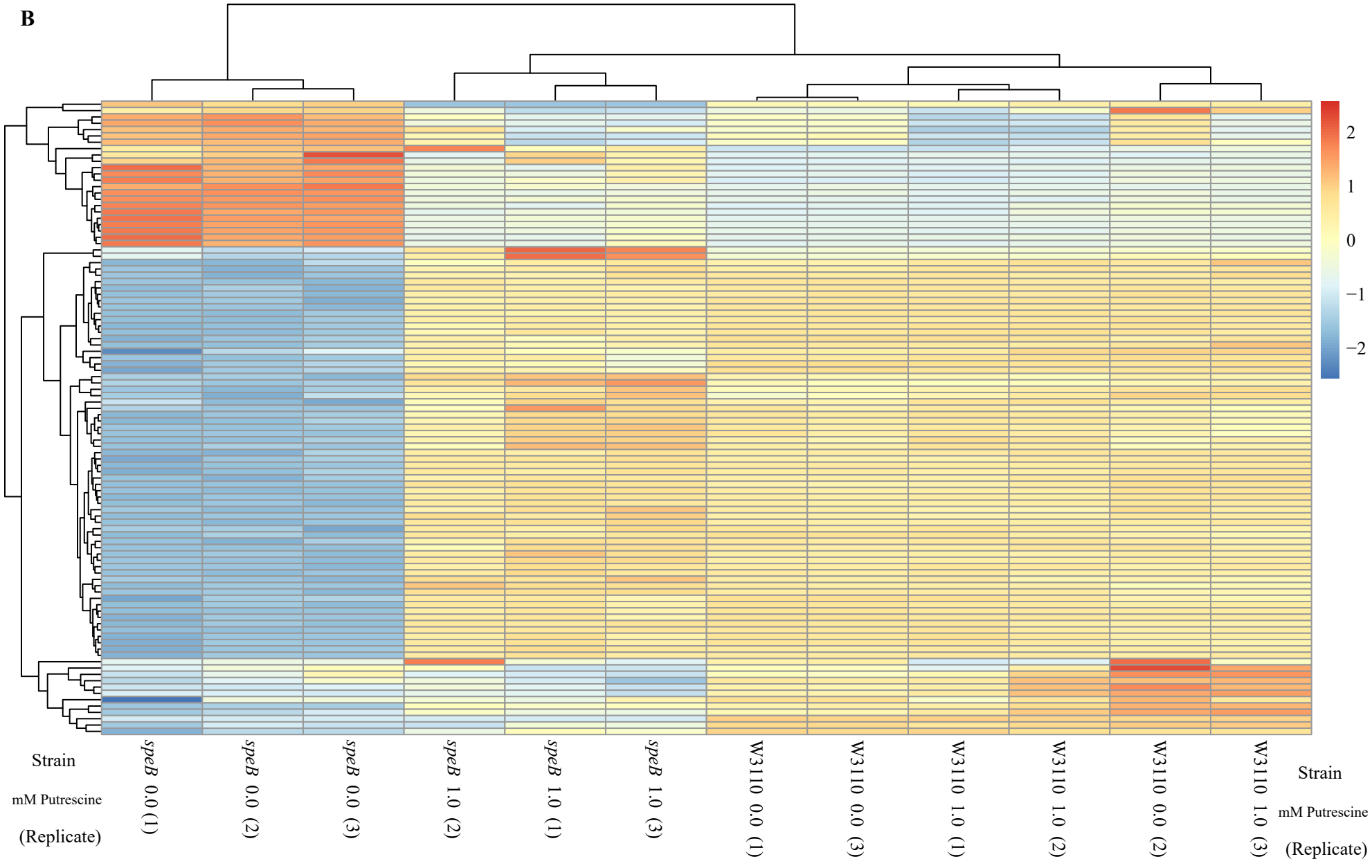
B
2
1
0
−1
−2
Strain
mM Putrescine
(Replicate)
speB 0.0 (1)
speB 0.0 (2)
speB 0.0 (3)
speB 1.0 (2)
speB 1.0 (1)
speB 1.0 (3)
W3110 0.0 (1)
W3110 0.0 (3)
W3110 1.0 (1)
W3110 1.0 (2)
W3110 0.0 (2)
W3110 1.0 (3)
Strain
mM Putrescine
(Replicate)

Figure 9 Legend

Figure 9: Visual representation of the results from transcriptomic sequencing of W3110 and the Δ*speB* mutant's gene expression in media with and without 1.0 mM putrescine. (A) Multidimensional scaling plot of the parental and Δ*speB* mutant transcriptomes. When grown with 1.0 mM putrescine (red), the Δ*speB* mutant transcriptome (triangles) are nearly identical to the parental transcriptomes when grown without and with putrescine (blue and red circles, respectively). When grown without putrescine, the Δ*speB* mutant transcriptome (blue triangles) is greatly skewed from transcriptomes of the parental strain and the Δ*speB* mutant grown with putrescine. (B) Heatmap of the top 100 most variable genes further demonstrates the distinctiveness of the Δ*speB* mutant grown without putrescine and the similarities of the Δ*speB* mutant transcriptome when grown with 1.0 mM putrescine supplementation and the parental grown with or without putrescine. In this figure the Δ*speB* mutant was J15.

Figure 10

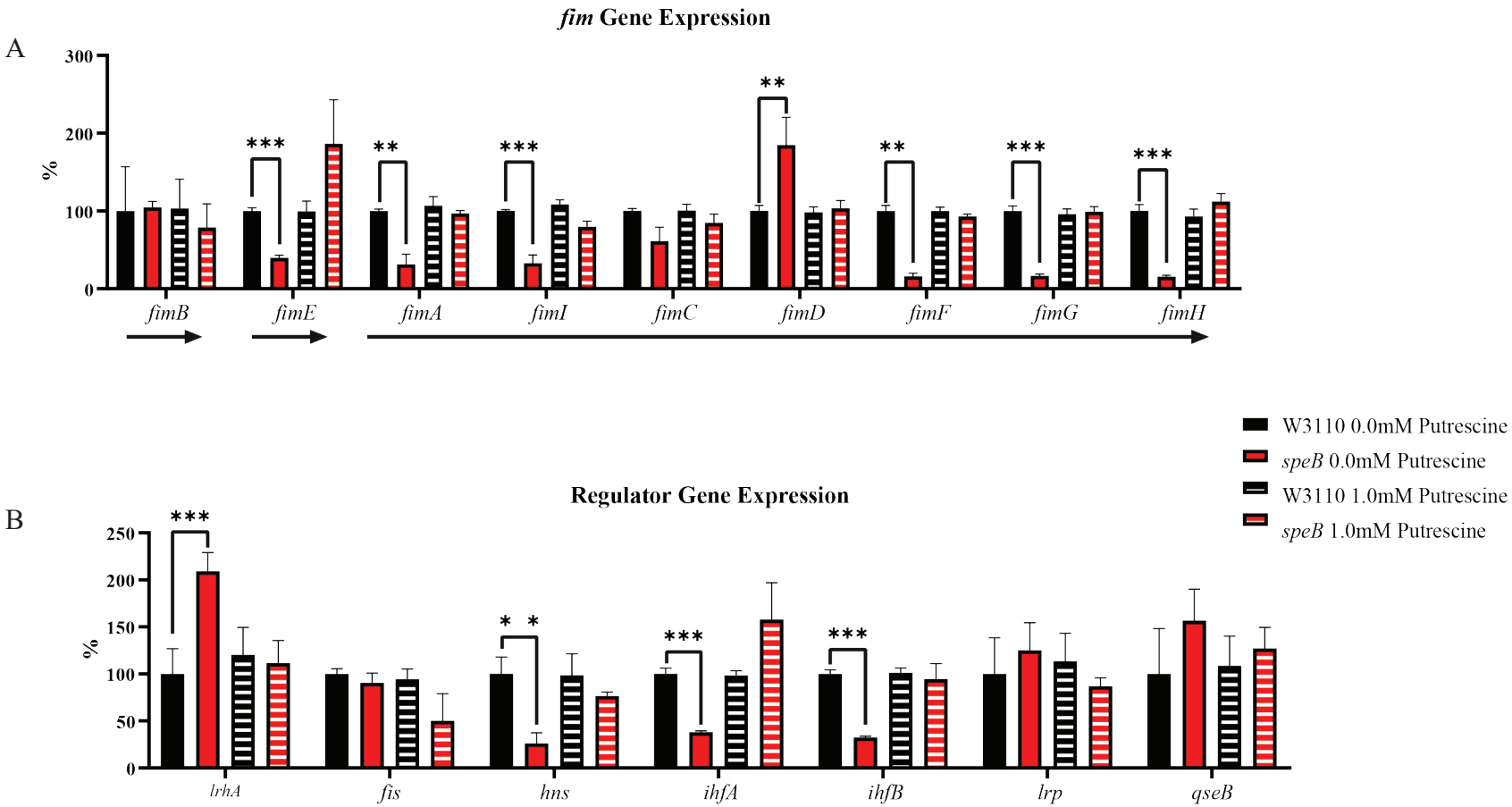

C

Surface Motility of Regulator Mutants

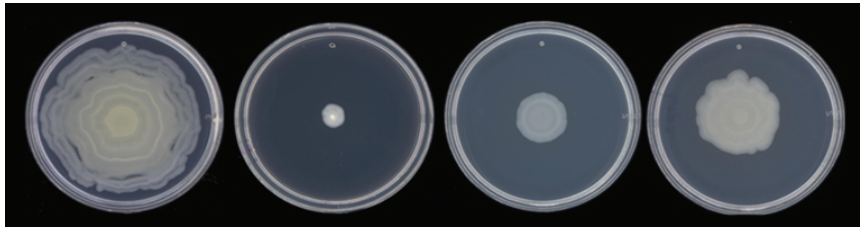

W3110 Δ*hns* Δ*ihfA* Δ*lrp*

D

Regulator Mutant Surface Motility Diameters

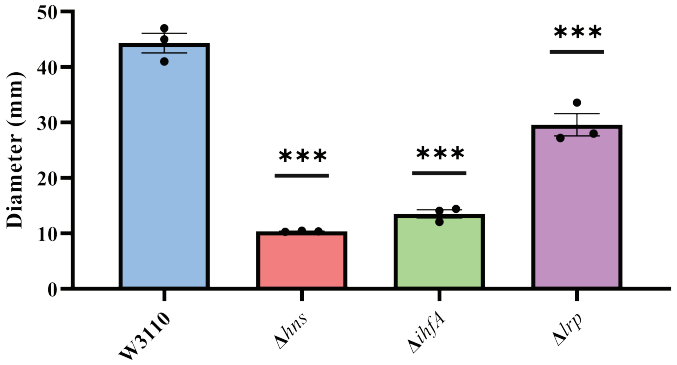

Figure 10 Legend

Figure 10: Transcriptomic sequencing of genes for the *fim* region and regulators that control *fim* gene expression. (A) Expression of the *fim* genes in the parental W3110 and the *speB* mutant with and without putrescine supplementation. Values were calculated by dividing the individual replicates' counts per million (CPM) value for each gene by the mean CPM of that gene in W3110 grown without putrescine and multiplying by 100 to yield the percent expression. Arrows below the genes signify the known operons: *fimB* and *fimE* belong to single gene operons, while *fimAICDFGH* belong to one operon. One way ANOVA was used to determine significance using Dunnett hypothesis testing. **, $p < 0.01$; ***, $p < 0.001$. (B) Expression of some regulators known to affect *fim* gene expression. Values were calculated as described in (A). ***, $p < 0.001$. (C) Surface motility of W3110 and three regulator mutants (Δ*hns*, Δ*ihfA*, and Δ*lrp*). A gene found to be significantly different by this transcriptomic analysis (*hns*) was confirmed to be important in surface motility. In this figure the Δ*speB* mutant was J15. (D) Diameter of surface movement of regulatory mutants after 36 hours. Error bars represent standard deviations for three independent replicates. Statistical analysis was performed using the Dunnett test of significance: *, $P<0.05$; **, $P<0.01$; ***, $P<0.001$. All assays were performed in triplicate.

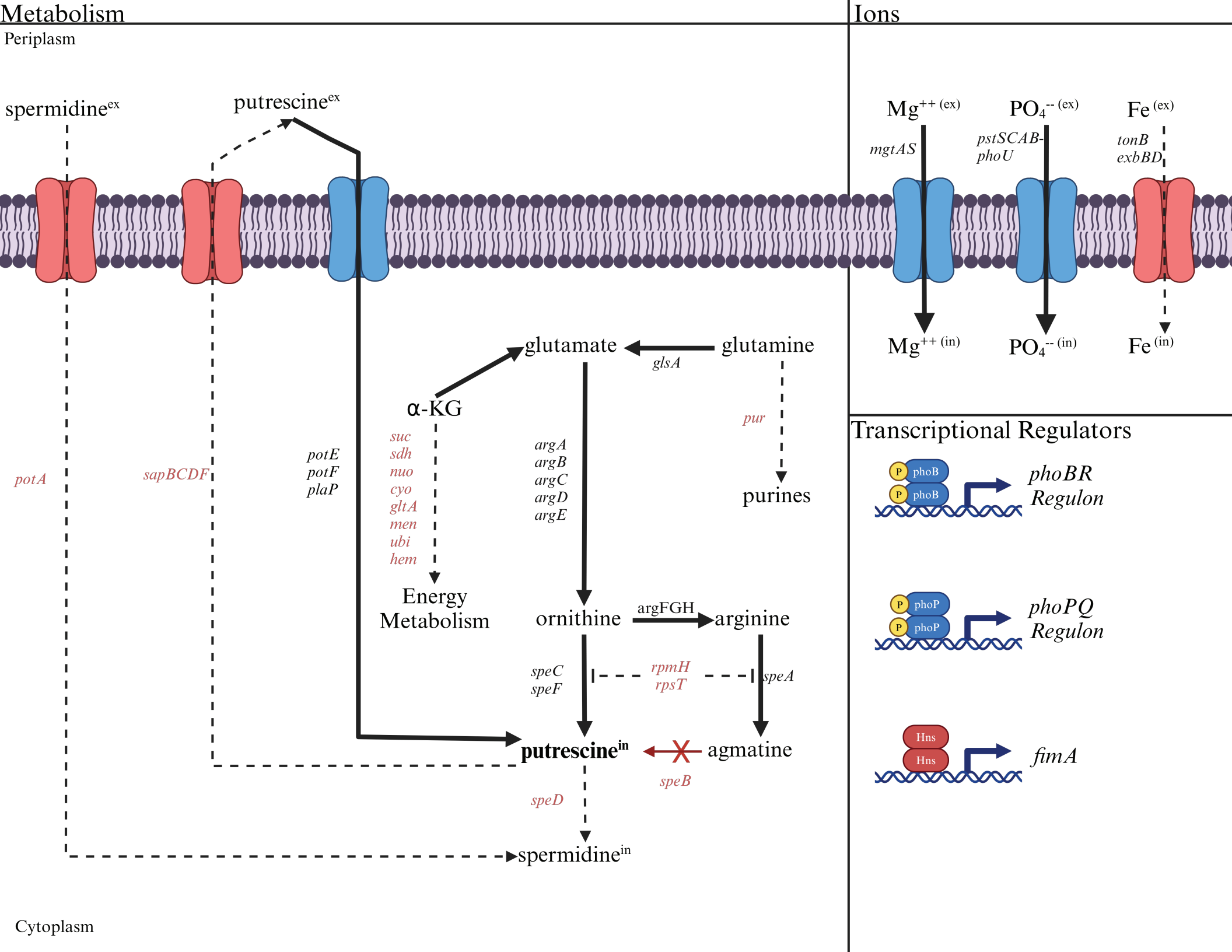
Metabolism
Ions
Periplasm
spermidine^ex
putrescine^ex
Mg++ (ex)
PO4-- (ex)
Fe (ex)
mgtAS
pstSCAB-
phoU
tonB
exbBD
Mg++ (in)
PO4-- (in)
Fe (in)
glutamate
glutamine
glsA
α-KG
pur
purines
potA
sapBCDF
potE
potF
plaP
suc
sdh
nuo
cyo
gltA
men
ubi
hem
argA
argB
argC
argD
argE
Energy
Metabolism
ornithine
argFGH
arginine
speC
speF
rpmH
rpsT
speA
putrescine^in
agmatine
speB
speD
spermidine^in
Cytoplasm
Transcriptional Regulators
P
phoB
phoB
phoBR
Regulon
P
phoP
phoP
phoPQ
Regulon
Hns
Hns
fimA

Figure 11 Legned

Figure 11: The deduced diversion of metabolism in a *speB* mutant away from energy metabolism toward putrescine synthesis compared to the parental strain. The effects of low putrescine are shown. Genes and processes (transport and transcriptional regulators) in red have fewer transcripts, while those in black or blue have more. The dashed lines represent proposed reduction in metabolic flux because of fewer transcripts from genes coding for the enzymes involved. Operons are shown except for the larger operons or regulons. For example, *pur* is meant to represent the unlinked genes that code for enzymes of purine synthesis. Table 2 or Supplemental Table 1 should be consulted for specific genes and the quantitative change in transcripts.